

Spring 2014

# Exhaust Thermal Management Using Cylinder Deactivation and Late Intake Valve Closing

Mark E. Magee  
*Purdue University*

Follow this and additional works at: [https://docs.lib.purdue.edu/open\\_access\\_theses](https://docs.lib.purdue.edu/open_access_theses)



Part of the [Mechanical Engineering Commons](#)

---

## Recommended Citation

Magee, Mark E., "Exhaust Thermal Management Using Cylinder Deactivation and Late Intake Valve Closing" (2014). *Open Access Theses*. 214.

[https://docs.lib.purdue.edu/open\\_access\\_theses/214](https://docs.lib.purdue.edu/open_access_theses/214)

This document has been made available through Purdue e-Pubs, a service of the Purdue University Libraries. Please contact [epubs@purdue.edu](mailto:epubs@purdue.edu) for additional information.

**PURDUE UNIVERSITY**  
**GRADUATE SCHOOL**  
**Thesis/Dissertation Acceptance**

This is to certify that the thesis/dissertation prepared

By Mark E. Magee

Entitled

Exhaust Thermal Management Using Cylinder Deactivation and Late Intake Valve Closing

For the degree of Master of Science in Mechanical Engineering

Is approved by the final examining committee:

Gregory M. Shaver

Chair

Peter H. Meckl

Robert P. Lucht

To the best of my knowledge and as understood by the student in the *Research Integrity and Copyright Disclaimer (Graduate School Form 20)*, this thesis/dissertation adheres to the provisions of Purdue University's "Policy on Integrity in Research" and the use of copyrighted material.

Approved by Major Professor(s): Gregory M. Shaver

Approved by: David Anderson

Head of the Graduate Program

12/11/2013

Date

EXHAUST THERMAL MANAGEMENT USING CYLINDER DEACTIVATION  
AND LATE INTAKE VALVE CLOSING

A Thesis

Submitted to the Faculty

of

Purdue University

by

Mark E. Magee

In Partial Fulfillment of the

Requirements for the Degree

of

Master of Science in Mechanical Engineering

May 2014

Purdue University

West Lafayette, Indiana

## ACKNOWLEDGMENTS

I would like to thank my advisor, Dr. Gregory M. Shaver, for giving me the opportunity to be a member of his team and work on such an interesting and exciting project. I also thank my other committee members, Dr. Peter Meckl and Dr. Robert Lucht, for their additional involvement and feedback.

Thank you to our sponsors at Cummins and Eaton including David Koeberlein, Ray Shute, Ed Koeberlein, Jim McCarthy, and Doug Nielsen for not only funding this work, but also providing their technical insight and experience. It has been invaluable.

I would also like to thank the technical shop staff at Herrick Laboratories, Bob Brown, Gil Gordon, Ron Evans, and Frank Lee, for all of their help, as well as Donna Cackley for helping placing orders, and making travel and meeting arrangements.

Thank you to my fellow team members David Fain, Leighton Roberts, Chuan Ding, Akash Garg, Aswin Karthik, and Lucius Wang for all of your assistance in helping me solve the most difficult problems.

A special thanks to Lyle Kocher and Ed Koberlein who answered many phone calls and emails filled with questions. I would not have accomplished what I have without your help and insight.

Finally, I would like to thank my family for supporting me throughout this endeavor. Their support and love helped me continue on in the most challenging times. I couldn't have done it without them.

## TABLE OF CONTENTS

	Page
LIST OF TABLES . . . . .	iv
LIST OF FIGURES . . . . .	v
ABSTRACT . . . . .	viii
1. INTRODUCTION . . . . .	1
1.1 Motivation . . . . .	1
1.2 Literature Review . . . . .	2
1.2.1 Current Aftertreatment Thermal Management Strategies . .	5
1.3 Experimental Set-Up . . . . .	9
1.4 Contributions . . . . .	13
1.5 Outline . . . . .	14
2. EFFECT OF CYLINDER DEACTIVATION ON EXHAUST GAS TEM- PERATURES . . . . .	16
2.1 Effect of Air to Fuel Ratio on Exhaust Gas Temperatures . . . . .	16
2.2 Effect of Cylinder Deactivation on AFR . . . . .	18
2.3 Load Sweeps at 1200RPM Utilizing CDA . . . . .	19
2.3.1 Exhaust Temperature Effects . . . . .	21
2.3.2 Engine Performance Effects . . . . .	23
3. EFFECT OF CYLINDER DEACTIVATION AND LATE INTAKE VALVE CLOSING ON EXHAUST GAS TEMPERATURES . . . . .	32
3.1 Effect of Opening VGT on AFR . . . . .	32
3.2 Effect of Cylinder Deactivation and LIVC on AFR . . . . .	32
3.2.1 Exhaust Temperature Effects . . . . .	34
3.2.2 Engine Performance Effects . . . . .	37
4. CYLINDER DEACTIVATION RANGE MEETING NOX EMISSION TAR- GETS . . . . .	43
4.1 Exhaust Temperature Effects . . . . .	43
4.2 Engine Performance Effects . . . . .	45
5. CONCLUSIONS AND FUTURE WORK . . . . .	51
5.1 Exhaust Gas Temperature Increase Projection across Operating Map	51
5.2 Summary and Future Work . . . . .	54
LIST OF REFERENCES . . . . .	59

## LIST OF TABLES

Table	Page
1.1 Nominal Engine Parameters. . . . .	10
2.1 Mechanical Operating Constraints. . . . .	20
3.1 Load Sweeps Performed. . . . .	34

## LIST OF FIGURES

Figure	Page
1.1 EPA and Euro Emissions Regulations for Heavy Duty [1]. . . . .	1
1.2 Exhaust Gas Temperature for a Cummins 6.7L ISB Engine. . . . .	3
1.3 Aftertreatment System Used with a Cummins ISV Engine. . . . .	4
1.4 NOx Conversion Efficiency vs. Catalyst Temperature [5]. . . . .	5
1.5 Schematic of a Modern Diesel Engine. . . . .	11
1.6 Picture of Experimental Engine Setup. . . . .	12
1.7 Schematic of Variable Valve Actuation System. . . . .	13
2.1 Adabatic Flame Temperature as a Function of Air to Fuel Ratio. . . .	17
2.2 Experimental Turbine Outlet Temperature vs. Air to Fuel Ratio. . . .	18
2.3 Turbine Outlet Temperature vs. Torque at 1200 RPM in Cylinder Deactivation. . . . .	21
2.4 Turbine Inlet Temperature vs. Torque at 1200 RPM in Cylinder Deactivation. . . . .	22
2.5 Air to Fuel Ratio vs. Torque at 1200 RPM in Cylinder Deactivation. . .	23
2.6 Airflow vs. Torque at 1200 RPM in Cylinder Deactivation. . . . .	24
2.7 Normalized Brake Thermal Efficiency at 1200 RPM in Cylinder Deactivation. . . . .	25
2.8 LogP-LogV Diagram - Gross Indicated Mean Effective Pressure, GIMEP.	26
2.9 LogP-LogV Diagram - Net Indicated Mean Effective Pressure, NIMEP.	26
2.10 LogP-LogV Diagram - Pumping Mean Effective Pressure, PMEP. . . .	27
2.11 Normalized Open Cycle Efficiency at 1200 RPM in Cylinder Deactivation.	28
2.12 PMEP at 1200 RPM in Cylinder Deactivation. . . . .	29
2.13 Normalized Closed Cycle Efficiency at 1200 RPM in Cylinder Deactivation. . . . .	30
2.14 Main Injection Timing at 1200 RPM in Cylinder Deactivation. . . . .	31

Figure	Page
3.1 Volumetric Efficiency vs. Intake Valve Close Timing. . . . .	33
3.2 Turbine Outlet Temperature vs. Torque at 1200 RPM in Cylinder Deactivation and LIVC. . . . .	35
3.3 Air to Fuel Ratio vs. Torque at 1200 RPM in Cylinder Deactivation and LIVC. . . . .	36
3.4 AirFlow vs. Torque at 1200 RPM in Cylinder Deactivation and LIVC. . . . .	36
3.5 Volumetric Efficiency vs. Torque at 1200 RPM in Cylinder Deactivation and LIVC. . . . .	37
3.6 Normalized BTE vs. Torque at 1200 RPM in Cylinder Deactivation and LIVC. . . . .	38
3.7 Normalized OCE vs. Torque at 1200 RPM in Cylinder Deactivation and LIVC. . . . .	39
3.8 PMEP vs. Torque at 1200 RPM in Cylinder Deactivation and LIVC. . . . .	39
3.9 IMP vs. Torque at 1200 RPM in Cylinder Deactivation and LIVC. . . . .	40
3.10 Normalized CCE vs. Torque at 1200 RPM in Cylinder Deactivation and LIVC. . . . .	40
3.11 ECR vs. Torque at 1200 RPM in Cylinder Deactivation and LIVC. . . . .	41
3.12 BSNOX vs. Torque at 1200 RPM in Cylinder Deactivation and LIVC. . . . .	42
4.1 TOT vs. Torque at 1200 RPM in Cylinder Deactivation with NOx Targets. . . . .	44
4.2 TIT vs. Torque at 1200 RPM in Cylinder Deactivation with NOx Targets. . . . .	45
4.3 AFR vs. Torque at 1200 RPM in Cylinder Deactivation with NOx Targets. . . . .	46
4.4 Air Flow vs. Torque at 1200 RPM in Cylinder Deactivation with NOx Targets. . . . .	47
4.5 Normalized BTE vs. Torque at 1200 RPM in Cylinder Deactivation with NOx Targets. . . . .	48
4.6 Normalized OCE vs. Torque at 1200 RPM in Cylinder Deactivation with NOx Targets. . . . .	48
4.7 EMP vs. Torque at 1200 RPM in Cylinder Deactivation with NOx Targets. . . . .	49



Figure	Page
4.8 Normalized CCE vs. Torque at 1200 RPM in Cylinder Deactivation with NOx Targets. . . . .	49
4.9 SOI vs. Torque at 1200 RPM in Cylinder Deactivation with NOx Targets.	50
4.10 FSN vs. Torque at 1200 RPM in Cylinder Deactivation with NOx Targets.	50
5.1 Exhaust Gas Temperature for a Cummins 6.7L ISB Engine. . . . .	52
5.2 AFR for a Cummins 6.7L ISB Engine. . . . .	53
5.3 Experimental Turbine Outlet Temperature vs. Air to Fuel Ratio. . . . .	54
5.4 Exhaust Gas Temperatures Utilizing CDA and LIVC for a Cummins 6.7L ISB Engine. . . . .	55
5.5 Improved BTE vs. Torque at 1200 RPM in Cylinder Deactivation with NOx Targets. . . . .	57

## ABSTRACT

Magee, Mark E. M.S.M.E., Purdue University, May 2014. Exhaust Thermal Management using Cylinder Deactivation and Late Intake Valve Closing. Major Professor: Gregory M. Shaver, School of Mechanical Engineering.

Progressively stricter emission regulations have compelled diesel engine manufacturers to develop new technologies that reduce harmful pollutants like NO<sub>x</sub> and soot. While manufacturers have previously been able to meet these regulations through the use of on engine technology such as exhaust gas recirculation and multiple pulse injections, exhaust after treatment systems such as diesel particulate filters and selective catalytic reduction systems have become necessary to meet recent stricter policies. While these after treatment systems are incredibly effective at reducing harmful emissions, to operate effectively the system needs to be above a certain temperature level typically between 250 and 300°C. Many methods such as additional fueling or electrical heaters have been explored and used to increase the temperature of the exhaust gases passing through these systems to heat them faster or maintain temperature.

The effect of cylinder deactivation, CDA, and late intake valve closing, LIVC, on raising exhaust gas temperatures was studied by performing load sweeps at 1200 RPM. The effect of CDA, CDA and LIVC, and CDA meeting specific NO<sub>x</sub> targets was analyzed. At low loads, CDA proved to be effective at raising exhaust temperature as well as providing an improvement in brake thermal efficiency, BTE. At higher loads, exhaust gas temperatures were also improved, but with a fuel consumption penalty. The introduction of LIVC in combination with CDA increased exhaust temperatures above 250°C, but did not improve BTE. The last sweeps, which targeted low NO<sub>x</sub> emissions, required the use of EGR and were able to raise temperatures above 250°C across all loads while meeting the targets. While meeting the targets, BTE was only improved at low loads.

The sweeps demonstrated that CDA and CDA combined with LIVC can be an extremely effective technology for raising exhaust gas temperatures even at low loads where exhaust temperatures are usually lowest. In many cases, an improvement in BTE can be accomplished as well.

## 1. INTRODUCTION

### 1.1 Motivation

With the growing concern over the effect of greenhouse gases on the environment, diesel engine emission regulations have become more stringent world wide. Organizations such as the United States Environmental Protection Agency, EPA, or the European Union, have further tightened these regulations each year as shown in Fig.1.1.

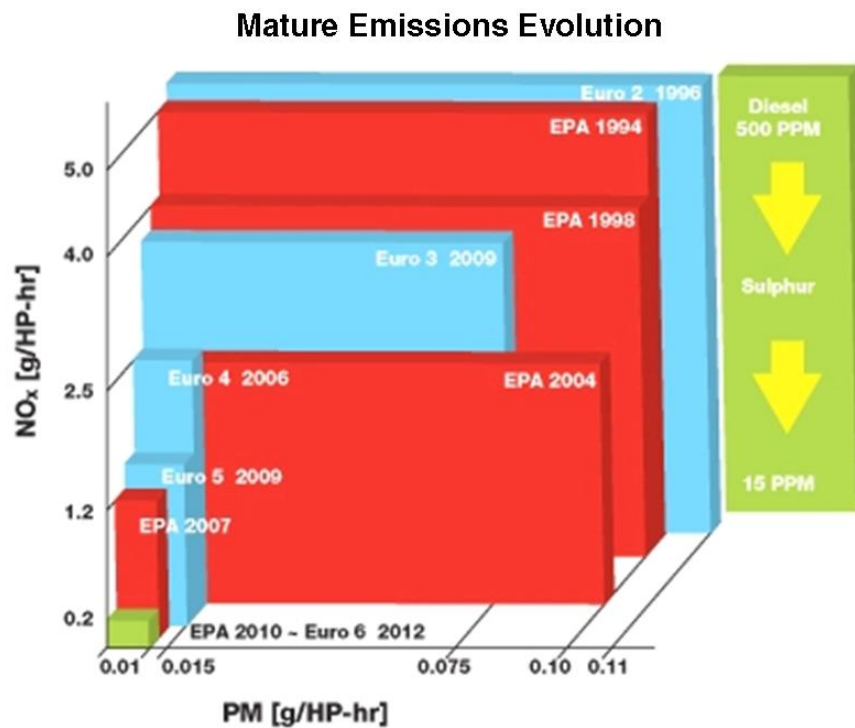


Figure 1.1. EPA and Euro Emissions Regulations for Heavy Duty [1].

These regulations govern the amount of carbon monoxide, CO, unburned hydrocarbons, HC, nitrogen oxides, NO<sub>x</sub> and particulate matter, PM. NO<sub>x</sub> and PM

emissions are notably higher in diesel engines than gasoline engines, and the reductions of these compounds remains a significant challenge in the engine manufacturing community. With previous, less restrictive regulations,  $\text{NO}_x$  and PM standards could be met through the use of in cylinder technology such as exhaust gas recirculation, EGR, and high pressure common rail injection systems. However, to meet the most recent requirements of  $\text{NO}_x$  and PM, the use of sophisticated aftertreatment systems is necessary.

To operate efficiently and effectively, these systems must be maintained at sufficiently high operating temperatures. The catalysts and other compounds used in the conversion process often need to be at temperatures above 250 or 300°C. However, at low load conditions such as idle, an engine cannot create sufficiently hot exhaust gases to heat up these systems. For example, the exhaust gas outlet temperature for a 6.7L Cummins ISB engine is shown in Fig. 5.1. Below the black line, temperatures are below 250°C. While it appears to only be a small portion of the map, through a drive cycle, an engine will spend a significant portion of its time in this lower region especially more urban applications like delivery trucks where there is frequent starting and stopping. In these low temperature situations, manufacturers currently use techniques such as additional fueling to increase the exhaust gas temperatures or electric heaters placed directly on the aftertreatment systems. However, a flexible valve system can be leveraged to modulate the airflow through the engine and increase exhaust temperatures by decreasing air to fuel ratio, AFR. This method of increasing exhaust gas temperatures can also possibly be done with no fuel penalty or even improve fuel consumption.

## 1.2 Literature Review

Most modern diesel engines come equipped with a sophisticated aftertreatment system consisting of some combination of a diesel particulate filter, DPF, diesel oxidation catalyst, DOC, lean  $\text{NO}_x$  trap, LNT, and selective catalytic reduction, SCR.

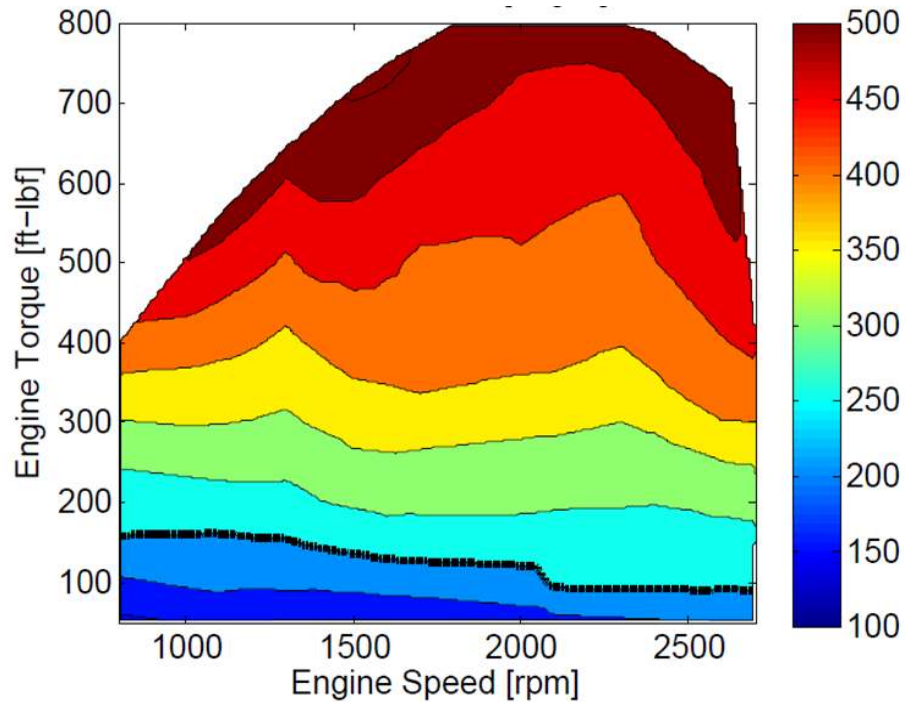


Figure 1.2. Exhaust Gas Temperature for a Cummins 6.7L ISB Engine.

Fig. 1.3 is an example of the system used with the Cummins ISV engine platform. A DPF is used to trap soot particles in a filter significantly reducing the tailpipe PM emissions; however, after a period of time, the filter can become clogged which causes excess back pressure on the engine. This degrades engine performance, and the process of regeneration is required. Passive regeneration relies on the temperature of the exhaust stream out of the engine to sufficiently oxidize the soot in the filter. In active regeneration, the exhaust temperature is increased through the use of additional fuel or other devices which when combined with excess oxygen in the exhaust will oxidize the soot particles in the filter. Active regeneration has become a commonly used process as a result of its controllability, but it also comes with a fuel penalty as very high temperatures on the order of 400 or 500°C are required for effective regeneration [2].

A DOC is used to reduce the hydrocarbon, carbon monoxide, and sulfur oxides produced by a diesel engine. With the assistance of various catalysts, the unburned hydrocarbons and CO react with the excess oxygen in the exhaust to produce CO<sub>2</sub>



Figure 1.3. Aftertreatment System Used with a Cummins ISV Engine.

and  $H_2O$  while similar reactions occur with the sulfur compounds in the exhaust to produce less harmful variants. The oxidation reactions inside the DOC are exothermic, and can significantly raise exhaust temperatures [3].

A lean  $NO_x$  trap and SCR system both aim to reduce the  $NO_x$  emissions of the engine. The high temperatures during diffusion combustion can produce large amounts of nitrogen oxides which have been shown to adversely affect the environment especially contributing to the formation of smog. While  $NO_x$  traps have proved effective in the past, with the extremely low regulations now enforced, the highly effective SCR systems are being used by many engine manufacturers. SCR systems rely on the injection of urea along with catalysts to convert  $NO_x$  to  $N_2$  and  $H_2O$ . While these systems are extremely effective, they must operate at temperatures typically above  $250^\circ C$  as shown in Fig.1.4. If the system is not operating at peak efficiency, the required  $NO_x$  emissions will not be met. In addition, if there is not sufficient temperature in the exhaust stream, when the urea is injected, it will not fully vaporize, and deposit directly on to the catalyst potentially producing more harmful emissions [4], As shown previously, a diesel engine often operates at speeds and loads where the

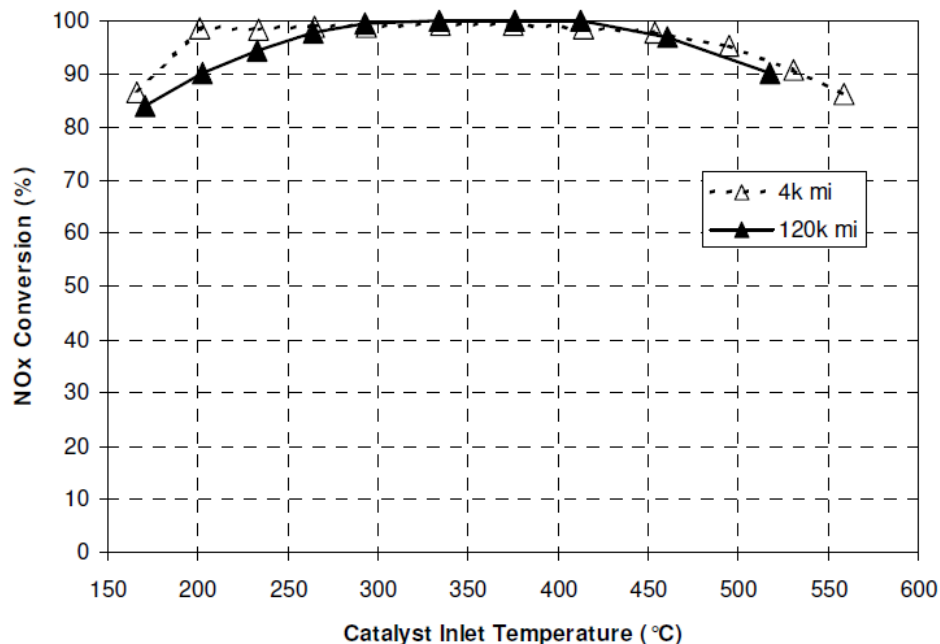


Figure 1.4. NOx Conversion Efficiency vs. Catalyst Temperature [5].

temperature of the exhaust does not meet the requirements for the aftertreatment systems discussed above. Therefore, a significant effort has been made to create strategies that can be used to heat up the catalysts faster or maintain the required temperatures.

### 1.2.1 Current Aftertreatment Thermal Management Strategies

Bouchez and Dementhon [6] investigated several strategies to increase exhaust temperatures in a multi cylinder diesel engine for regeneration of a diesel particulate trap. In cases where there was little EGR present nominally, increasing the amount of EGR flow was shown to be extremely effective in increasing exhaust gas temperatures. Increasing the amount of EGR in cylinder decreased the amount of air trapped in cylinder which increases exhaust temperatures. Opening the turbocharger waste gate was also found to be effective as a result of decreasing AFR. By opening the waste gate, less energy is supplied to the turbine which reduces the amount of air driven by the



compressor through the engine. They also used retarded injection timing as a means to increase exhaust temperatures, but this came with a fuel consumption penalty associated with late injections. Lastly, a post injection coupled with a diesel oxidation catalyst, DOC, raised the temperature of the gases entering the DPF. The post injection resulted in an increase in hydrocarbon concentration, which upon entering the DOC, the exothermic reaction further heated the exhaust gases.

Parks et. al. [7] also explored the use of in cylinder methods for aftertreatment thermal management composed of a DOC and DPF. The methods included additional fuel injected early and late in the combustion process across all cylinders and in only one cylinder, and injection of fuel directly into the exhaust stream. Each process was conducted on a DPF whose temperature was 150 or 300°C. They found that at 150°C the injection of extra fuel early in the combustion cycle slightly increased exhaust temperatures. However, with the system at such low temperatures, the DOC was unable to oxidize the fuel injection late in cylinder or in the exhaust pipe. With the aftertreatment system at 300°C, all of the methods were effective in raising exhaust temperatures with the largest increase seen with injection of fuel directly upstream of the DOC. In all cases, fuel penalties were observed with the highest penalties associated with additional fuel introduced into the system.

Singh et. al. [8] used post injections and upstream fuel injection to improve exhaust thermal management. Late post injections proved effective in raising the exhaust temperatures especially at high load, but early post injections did not have a significant effect. As in [7], the late post injection delivered additional hydrocarbons to the DOC. Using upstream fuel injection in the exhaust system, the resulting oxidation increased exhaust temperatures as shown in.

Singh et. al. [8] studied injecting fuel upstream of a DOC to increase exhaust temperatures before a DPF as a means of active regeneration. When the excess fuel reaches the DOC, the hydrocarbons are oxidized, and the exothermic nature of the reaction can cause a large increase in exhaust temperatures. Utilizing a Cummins ISM engine, this process was conducted with a DPF loaded with various amounts of

soot ranging from 1.1 to 4 g/L. When the fuel was injected upstream of the DOC, the resultant increase in exhaust temperatures was able to produce a 99% conversion efficiency in the DPF. While this method demonstrates another effective technique in increasing exhaust temperatures, the additional injection of fuel comes with a fuel consumption penalty for the vehicle.

Kim et. al. [9] used an electrical heater to improve cold start performance of DOC, SCR, and DPF aftertreatment system. The resistive heater was directly upstream of the DOC in an effort to increase the DOC catalyst temperature more quickly so that additional hydrocarbon oxidation could be used to heat the SCR. The system used the additional hydrocarbon injection to reduce the time required to heat up the SCR during start up. The electrical heater was used to increase the DOC temperature to 250°C which was the minimum temperature for hydrocarbon injection. As expected the amount of temperature increase was proportional to the power given to the electrical heating system and was able to reduce the time needed for warm up. Pfahl et.al. [10] also used electrical heating to improve cold start performance and were able to produce similar results reducing the heat up time of the DOC by 100 seconds. Akiyoshi et. al. [11] used a burner fed by vehicle fuel placed upstream of the aftertreatment system as another method to directly increase exhaust temperatures.

Cavina et. al. [12] swept start of main injection to determine the direct effect on exhaust gas temperatures. As injection timing was increased, exhaust temperatures increased with a maximum of 50°C when injection was advanced 15 degrees, but the advanced timing also increased fuel consumption as much as 15%.

Honardar et. al. [13] used main injection timing and increased post injection quantity at warm and cold conditions. At warm conditions, when main injection was placed later in the cycle, a 30°C increase in exhaust gas temperature was observed but came with a penalty in fuel consumption. At cold conditions meant to mimic start-up, an increase of approximately 80°C was achieved; however, there was a more severe fuel consumption penalty than during warm conditions likely due to inefficient combustion. At warm conditions, the use of an increased post injection

resulted in significantly higher exhaust temperatures. The maximum post injection quantity could improve temperatures by almost 200°C, but there is a direct decrease in efficiency corresponding to the additional fueling used in the post injection. At the cold conditions, only a 180°C improvement could be achieved.

An effective method for raising exhaust temperatures is reducing the air to fuel ratio of the engine which can be achieved through the use of a VGT, variable valve systems, or direct use of an intake throttle. Cavina et. al. [12] used VGT modulation, and intake throttling to improve thermal management. By opening the VGT, it was observed that exhaust temperatures could be raised resulting from a reduction in air to fuel ratio. When the VGT was opened 30%, a 30°C increase was observed, and unlike injection timing, open the VGT improved fuel consumption up to 6%. This improvement came from a reduction in pumping work. Using an intake throttle reduced AFR much like opening the VGT which produced a maximum temperature increase of 40°C. Intake throttling improved fuel consumption by as much as 15% by again reducing the pumping work.

Mayer et. al. [14] investigated the use of intake throttling as a means for DPF regeneration. A throttle was placed at various locations in the engine air path as a means to decrease the air to fuel ratio and increase exhaust gas temperatures. When the throttle is placed before the compressor inlet, exhaust gas temperatures were increased to 750K from temperatures as low as 450K, but with a fuel consumption penalty as a result of increased pumping work. Similar results were observed when the throttle was placed after the compressor. Finally, a throttle was placed before the turbine of the turbocharger, and while there was an increase in exhaust temperatures, there was also a more severe fuel consumption penalty, and also concern about increased temperature of engine components which could lead to engine damage.

Huang et. al. [15] used intake throttling to improve cold start performance of an aftertreatment system. At idle, a throttle was closed 90% of the way and was able to increase turbine inlet temperatures from approximately 175°C up to 190°C. With the addition of a retarded main injection, turbine inlet temperatures were increased

farther to approximately 215°C. Honardar et. al. [13] used a throttle directly after the compressor outlet to modulate airflow through the engine were able to increase exhaust temperatures by as much as 35°C in both warm and cold conditions; however, the increased intake manifold pressure caused by the throttle increased pumping work, reducing efficiency.

Gehrke et. al. [16] using a variable valve actuation system on a single cylinder engine and were able to increase exhaust temperatures by 60K using early intake valve timing and 120K using late intake valve closing with minimal fuel consumption penalties. LIVC produces higher exhaust temperatures as a result of the heating of charge in the intake manifold. By closing the intake valve later, some of the heated charge in the cylinder gets pushed back into the intake manifold. Both cases reduced the air to fuel ratio raising exhaust gas temperatures. Early exhaust valve opening was also examined and it could also raise exhaust temperatures, but there was a fuel consumption penalty as a result of lost expansion work.

While many studies such as [17], [18–20] have considered the implementation and fuel economy benefits of CDA, very few have explored the use of cylinder deactivation as a means of increasing exhaust gas temperatures. In addition, a large majority of the development has been for spark ignition engine platforms with little development targeted toward diesel engines.

### 1.3 Experimental Set-Up

The experiments presented were performed on a Cummins 2010 6.7L ISB engine. As shown in Fig.1.5, it is an in-line six cylinder engine with four valves per cylinder, and a geometric compression ratio of 17.3:1. The engine comes equipped with a high pressure cooled EGR system, and a variable geometry turbocharger, VGT. These two systems in combination control the amount of fresh air and EGR delivered to the cylinders. For this set of experiments, the VGT was downsized to increase air flow control authority at lower speeds and loads. The engine also comes equipped with

Table 1.1. Nominal Engine Parameters.

Parameter	Value	Units
No. of Cylinders	6	—
Valves per Cylinder	4	—
Firing Order	1,5,3,6,2,4	—
Maximum Injection Pressure	1800	bars
Bore Diameter	107	mm
Stroke	124	mm
Connecting Rod Length	192	mm
Compression Ratio	17.3	—
Intake Valve Opening	340 aTDC	CAD
Intake Valve Closing	565 aTDC	CAD
Exhaust Valve Opening	200 bTDC	CAD
Exhaust Valve Closing	20 aTDC	CAD
Intake Valve Diameter	29.27	mm
Exhaust Valve Diameter	29.4	mm



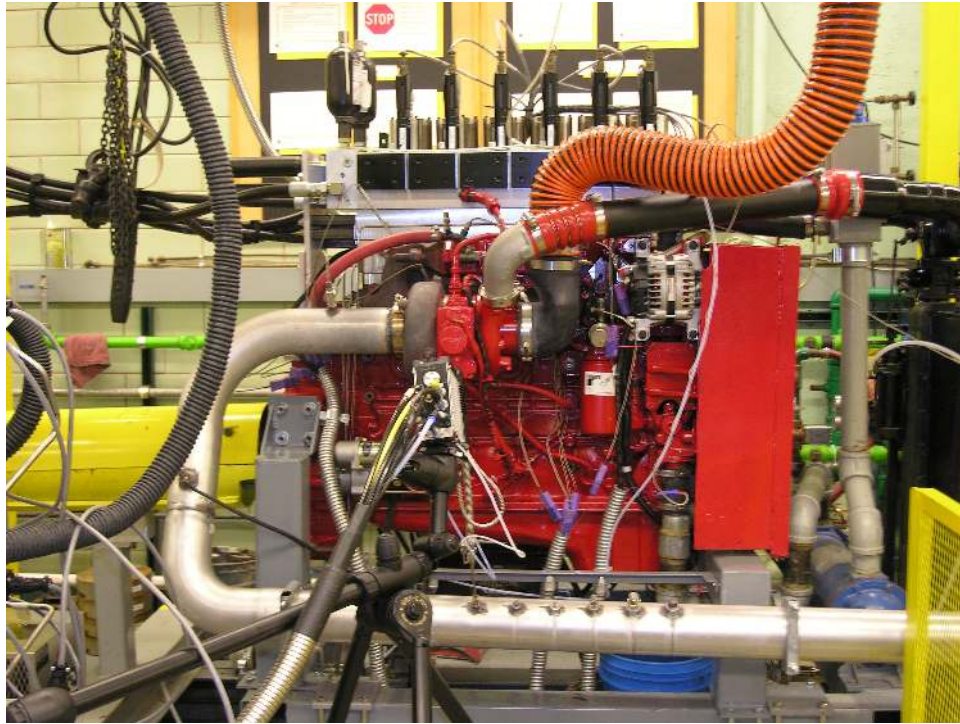


Figure 1.6. Picture of Experimental Engine Setup.

The experimental engine data is acquired using a dSPACE system. The dSPACE system collects data from the engine electronic control module, ECM, such as the fueling and timing commands as well as ECM sensor measurements. The ECM data is gathered from an open architecture ECM that allows direct read and write access to the memory locations. The dSPACE system also collects data from additional temperature, pressure, flow and emissions measurements instrumented on the engine test bed. Fresh air mass flow rate is measured using a laminar flow element, LFE, device. The engine charge flow is calculated using the LFE fresh air flow measurement and the measured EGR fraction. Emission gas analyzers are used to measure the composition of the exhaust gases as well as the concentration of  $\text{CO}_2$  in the intake manifold. Combustion NDIR Fast  $\text{CO}_2$  analyzers were utilized during this testing. EGR fraction is computed using the intake and exhaust manifold  $\text{CO}_2$  measurements.

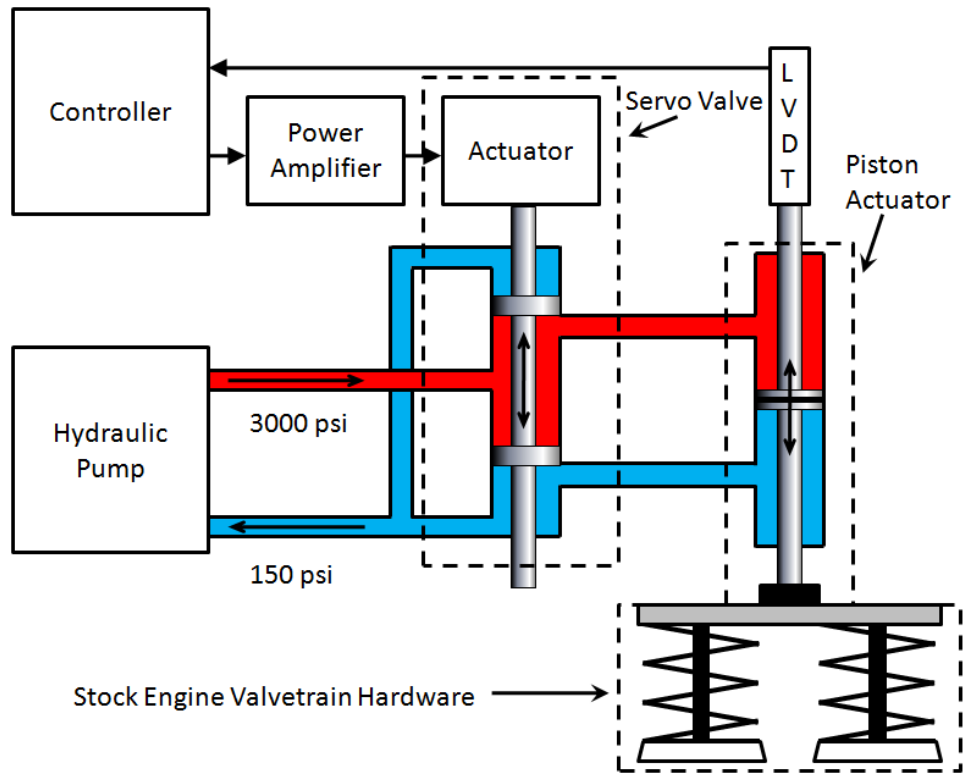


Figure 1.7. Schematic of Variable Valve Actuation System.

An universal exhaust gas oxygen (UEGO) sensor is mounted in the exhaust pipe shortly after the turbine outlet as shown in Fig. 1.5.

To implement CDA, the fueling is cut from cylinders 4, 5, and 6. Then the intake and exhaust valves are shut such that fresh charge is trapped in the cylinder. However, as the engine runs, since the piston rings do not create a perfect seal, the charge leaks past the rings. In order to keep oil from being drawn into the cylinder, the intake valve is opened every 100 cycles to recharge the cylinder and maintain positive pressure.

#### 1.4 Contributions

Utilizing a fully flexible valve actuation system, the ability of cylinder deactivation and late intake valve closing to significantly increase exhaust gas temperatures



was experimentally demonstrated. Cylinder deactivation while typically applied to gasoline and other spark ignited engines was applied to a diesel engine platform for both efficiency improvements and exhaust thermal management. Additionally, late intake valve closing was applied to the active cylinders combining two novel engine operating technologies.

## 1.5 Outline

**Chapter 2: EFFECT OF CYLINDER DEACTIVATION ON EXHAUST GAS TEMPERATURES** examines the effect of cylinder deactivation on raising exhaust gas temperatures by air to fuel ratio reduction. Additionally, the effect of cylinder deactivation on engine efficiency is also examined. At 1200 RPM, a load sweep was conducted in cylinder deactivation mode, and then compared with standard engine operation at each load.

**Chapter 3: EFFECT OF CYLINDER DEACTIVATION AND LATE INTAKE VALVE CLOSING ON EXHAUST GAS TEMPERATURES** examines the combined effect of cylinder deactivation and late intake valve closing on raising exhaust gas temperatures by air to fuel ratio reduction. At 1200 RPM, load sweeps were conducted in cylinder deactivation mode with different LIVC timings, and then compared with standard engine operation at each load..

**Chapter 4: CYLINDER DEACTIVATION RANGE MEETING NO<sub>x</sub> EMISSION TARGETS** examines the operating capability of cylinder deactivation when meeting designated  $NO_x$  emission targets. These targets represent the engine out emission standards that would be expected of a production engine. At 1200 RPM, a load sweep was conducted in cylinder deactivation mode, and EGR was used to lower NO<sub>x</sub> emissions. The sweeps are then compared with standard engine operation at each load with similar NO<sub>x</sub> emissions.

**Chapter 5: CONCLUSIONS AND FUTURE WORK** projects the ability of CDA and LIVC to increase exhaust gas temperatures across the operating range of

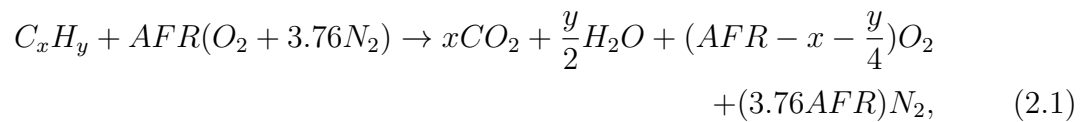
the engine. This projection helps to examine the capability of cylinder deactivation and late intake closing as an exhaust thermal management technique. Additionally, future work that would further the understanding of these technologies is described.

## 2. EFFECT OF CYLINDER DEACTIVATION ON EXHAUST GAS TEMPERATURES

A fundamental characteristic of conventional diesel engine operation is the control of load through fueling quantity only with no throttling applied to airflow through the engine. This leads to lean combustion environments especially at low loads where AFR can be as high as 80 or 100 at idle conditions. As a result, exhaust gas temperatures are well below the desired 250°C threshold as shown previously in Fig. 5.1. Cylinder deactivation and late intake valve closing can both be used to throttle airflow through the engine bringing AFR closer to stoichiometric conditions raising exhaust gas temperature.

### 2.1 Effect of Air to Fuel Ratio on Exhaust Gas Temperatures

Many factors affect exhaust gas temperatures including injection timing and rail pressure, the dominant factor is air to fuel ratio. The ratio of air and fuel drives the amount of heat release during the combustion reaction with the hottest temperatures occurring when the mixture is of stoichiometric proportions. When AFR equals one, the reaction is said to be stoichiometric and results in the highest product temperatures as shown in Eq.2.1,



which is the generic combustion reaction for a hydrocarbon fuel. Typically, the effect of AFR on product temperature is characterized by adiabatic flame temperature.

Assuming that the reaction occurs in a fully adiabatic system, the enthalpy of the reactants equals the enthalpy of the products as shown in Eq.2.2,

$$H_{Reactants} = H_{Products}. \quad (2.2)$$

Using the standard reference temperature of 298°K and using the lower heating value of the fuel in place of the heat of formation of products and reactants, Eq.2.2 can be rearranged to Eq.2.3,

$$\begin{aligned} LHV_{Fuel} = 3.76AFRC_{p,N_2}(T_f - 298) + (AFR - x - \frac{y}{4})C_{p,O_2}(T_f - 298) \\ + \frac{y}{2}C_{p,H_2O}(T_f - 298) + xC_{p,CO_2}(T_f - 298), \end{aligned} \quad (2.3)$$

where  $T_f$  is the adiabatic flame temperature. Using this relationship, the effect of AFR on adiabatic flame temperature is shown in Fig. 2.1, and it can be seen that as AFR decreases, adiabatic flame temperature increases. As the temperature during combustion in cylinder increases, the temperature of the exhaust products also increases. This relationship demonstrates why AFR is the parameter with the strongest effect on exhaust gas temperatures.

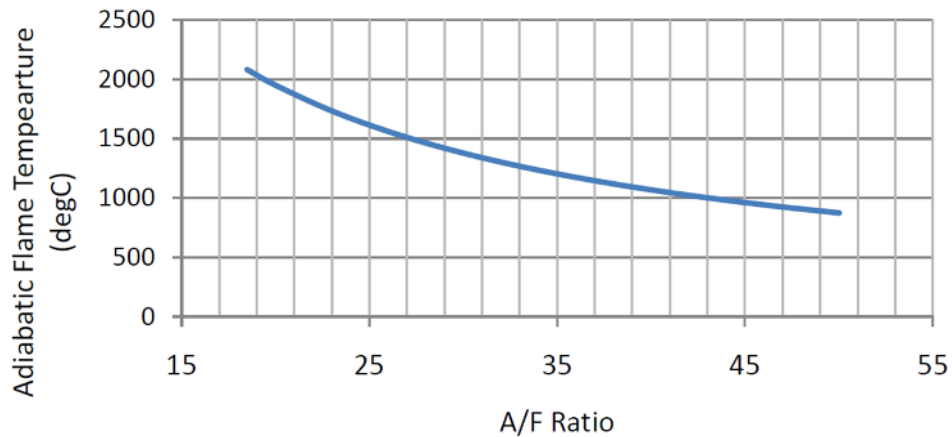


Figure 2.1. Adabatic Flame Temperature as a Function of Air to Fuel Ratio.

To further demonstrate the relationship between AFR and exhaust gas temperatures, experimental data was gathered across a variety of engine speeds and loads

and engine operating modes such as late intake valve closing, LIVC, early intake valve closing, EIVC, early exhaust valve opening, EEVO, and CDA. The data is shown in Fig. 5.3, and a monotonic relationship is apparent. The outliers are cases with very high EGR rates. The relationship between AFR and TOT can be approximated by

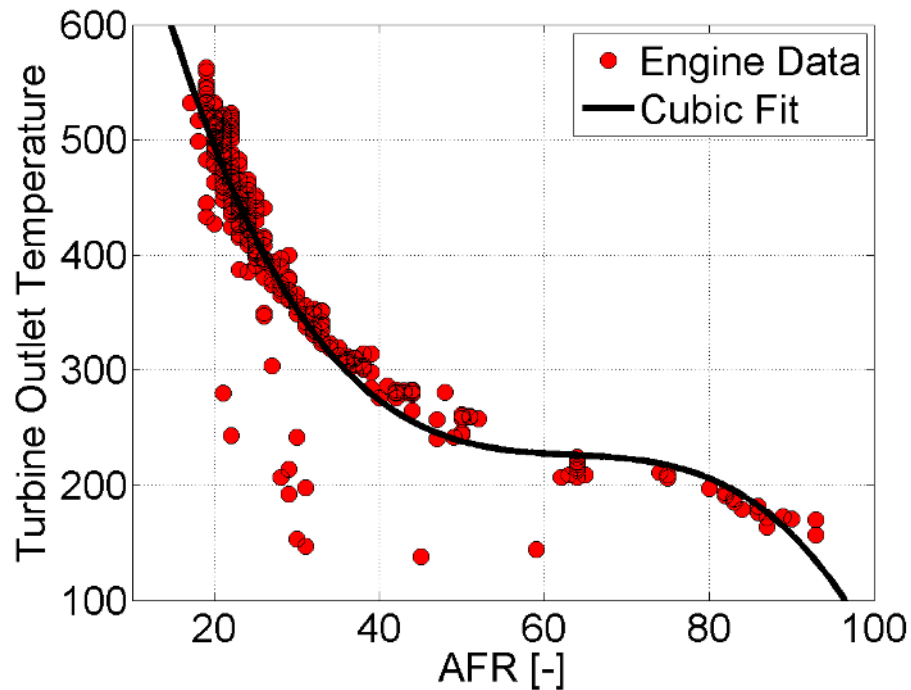


Figure 2.2. Experimental Turbine Outlet Temperature vs. Air to Fuel Ratio.

a third order polynomial, and while this is not a perfect fit, it allows for the approximation of trends resulting from AFR modulation as a result of CDA and LIVC.

## 2.2 Effect of Cylinder Deactivation on AFR

Air flow through an engine can be modeled by the speed density equation shown in Eq.5.2,

$$W_{air} = \frac{\eta_v P_{im} V_d N}{n R T_{im}}, \quad (2.4)$$

where  $W_{air}$  is the airflow through the engine,  $\eta_v$  is the volumetric efficiency of the engine,  $P_{im}$  is the intake manifold pressure,  $V_d$  is the engine displacement,  $N$  is the engine speed,  $n$  is the number of revolutions per cycle,  $R$  is the universal gas constant for air, and  $T_{im}$  is the intake manifold temperature. Cylinder deactivation is sometimes called variable displacement engine because when a number of cylinders are shut, the effective displacement is reduced to only the active cylinders. In the case of this study, where three of the six cylinders are shut, the engine displacement is halved. It can be seen by examining Eq.5.2 that if all the other terms are held constant and the engine displacement is halved, the total airflow through the engine is also halved.

At the same time, to maintain torque, the total fueling delivered to the engine remains the same with double the fuel entering the active cylinders. Therefore, if the total fueling to the engine is maintained, by reducing the airflow through the engine, the AFR is halved as well as shown in Eq.2.5,

$$AFR_{3Cylinder} = \frac{W_{air,3Cylinder}}{W_{fuel,3Cylinder}} = \frac{\frac{1}{2}W_{air,6Cylinder}}{W_{fuel,6Cylinder}}. \quad (2.5)$$

Using the previously established relationship between AFR and TOT, it can be shown that cylinder deactivation has a significant effect on increasing TOT.

### 2.3 Load Sweeps at 1200RPM Utilizing CDA

To study the effect of CDA outline above, at 1200RPM, beginning at 50ft-lbs, engine load was stepped by 50 ft-lbs until an engine limit was reached. These limits could be low AFR, high TIT, or a variety of other mechanical limitations summarized in Table2.1. Throughout the sweep, no EGR was used so that the effect of CDA and LIVC on the air flow process could be more clearly defined.

Table 2.1. Mechanical Operating Constraints.

Parameter	Value
Turbine Inlet Temperature	$< 760^{\circ}\text{C}$
Compressor Outlet Temperature	$< 230^{\circ}\text{C}$
Turbocharger Speed	$< 193 \text{ kRPM}$
Peak Cylinder Pressure	$< 2500 \text{ PSI}$
Exhaust Manifold Pressure	$< 120 \text{ inHg (gauge)}$
Pressure Rise Rate	$< 100 \text{ bar/sec}$

### 2.3.1 Exhaust Temperature Effects

The resulting turbine out temperatures from load sweep are shown in Fig. 2.3 as well as equivalent 6 cylinder operation temperatures. As shown, the maximum load able to be achieved in CDA at 1200RPM was 390 ft-lbs. At this point, the turbine inlet temperature reached the prescribed limit as shown in Fig. 2.4. As discussed previously, this increase in exhaust gas temperatures is driven by a decrease in AFR as shown in Fig. 2.5. At low loads such as 50 and 100 ft-lbs, air to fuel ratios are very high ranging between 90 and 50. This is a common occurrence in low load diesel operation where there is no standard regulation on airflow. These conditions correspond to the lowest TOT seen during engine operation whereas at higher loads, the margin for decreasing AFR is much smaller. At higher loads, AFR can already be as low as 20 or 25 which limits the maximum achievable load in cylinder deactivation. In Fig. 2.3, cylinder deactivation proves extremely effective in increasing TOT with

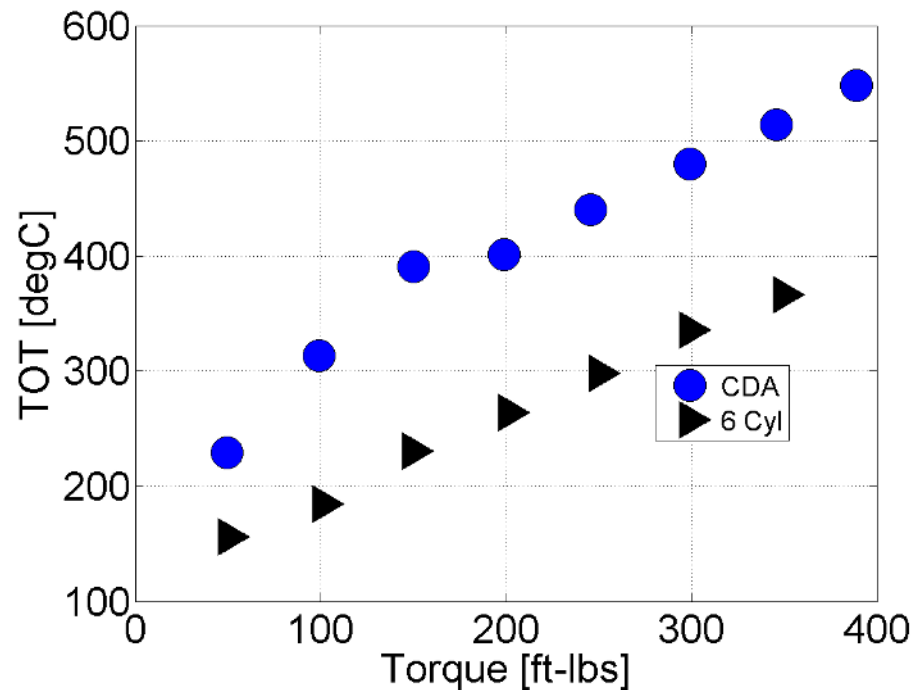


Figure 2.3. Turbine Outlet Temperature vs. Torque at 1200 RPM in Cylinder Deactivation.



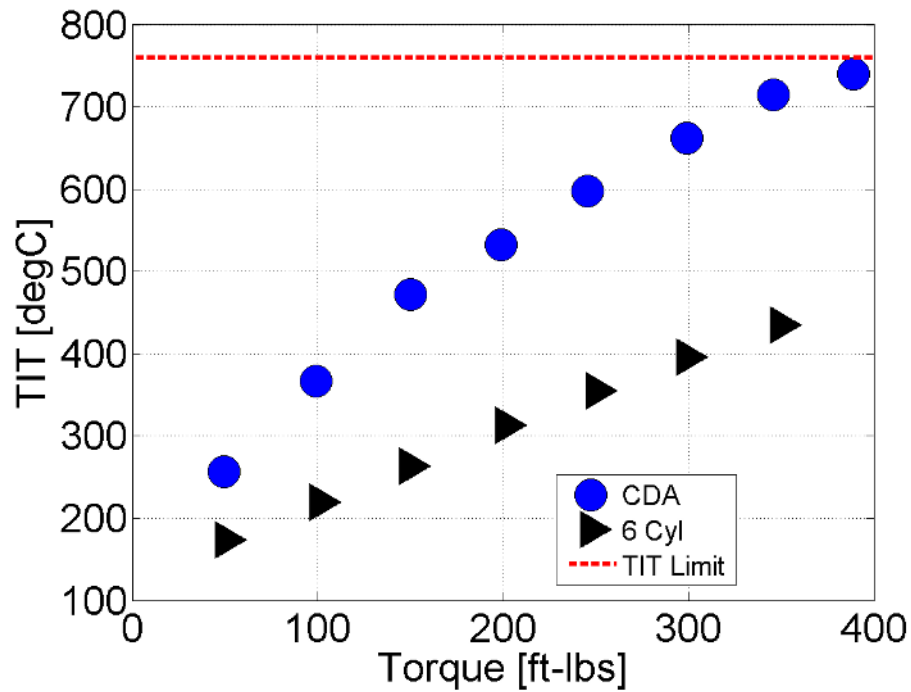


Figure 2.4. Turbine Inlet Temperature vs. Torque at 1200 RPM in Cylinder Deactivation.

a maximum increase of approximately  $150^{\circ}\text{C}$  at loads above 150 ft-lbs. The smallest increase in TOT is seen at 50 ft-lbs where CDA only produced approximately  $100^{\circ}\text{C}$  change. This discrepancy in TOT increase can be explained by examining the change in AFR in Fig. 2.5. At low loads, CDA reduces the AFR by half; however, the AFR is still too high to elicit large increases in combustion temperatures as shown previously in Fig. 2.1. At higher loads, the resulting AFR are sufficiently low that while it is a smaller relative change in AFR, a significant increase in TOT is achieved. From Eq.2.5, the decrease in AFR is caused by the reduction in engine displacement from 6 cylinders to 3 cylinders thereby reducing the airflow through the engine shown in Fig. 2.6. At low loads, the reduction in airflow is approximately half or even more in some cases; however, at higher loads there is a linear increase in airflow with load. This increase is a result of closing the variable geometry turbocharger to raise intake manifold pressure and drive more air into the cylinder. This was necessary to keep

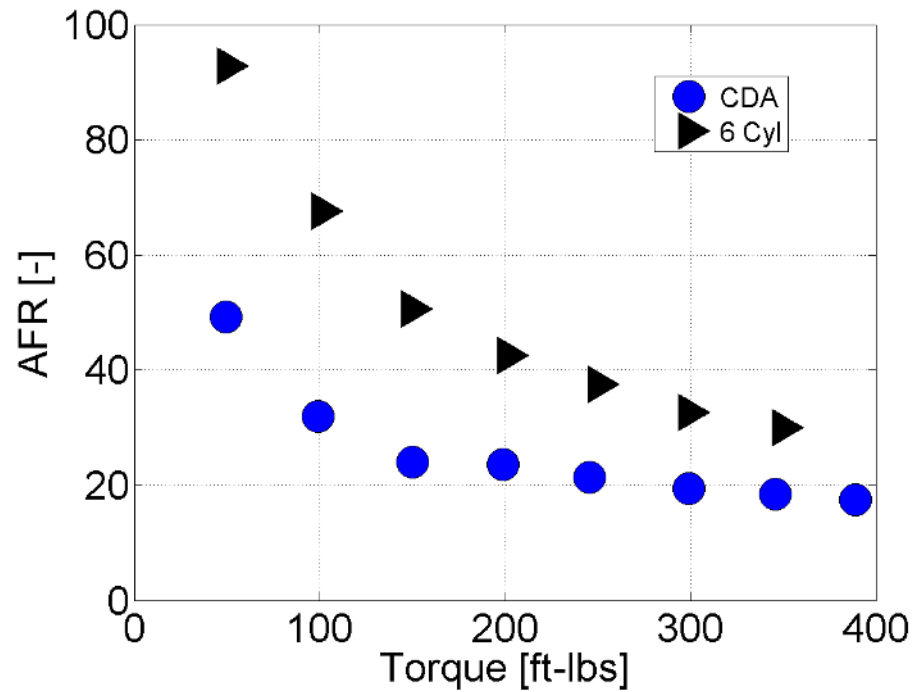


Figure 2.5. Air to Fuel Ratio vs. Torque at 1200 RPM in Cylinder Deactivation.

AFR from being reduced to far too a point where the engine would hit a mechanical constraint or run rich. In the case of 390 ft-lbs, the VGT was leveraged as far as possible, but there was no longer sufficient authority to increase airflow to keep TIT low.

### 2.3.2 Engine Performance Effects

Another important aspect of evaluating engine performance during CDA is the changes in thermal efficiency of the engine. While increasing thermal energy entering the after treatment is the primary goal of this study, maintaining or improving the thermal efficiency of the engine is always a target for novel engine technologies. Brake thermal efficiency, BTE, is defined as

$$BTE = \frac{FuelPower_{in}}{BrakePower_{out}}, \quad (2.6)$$

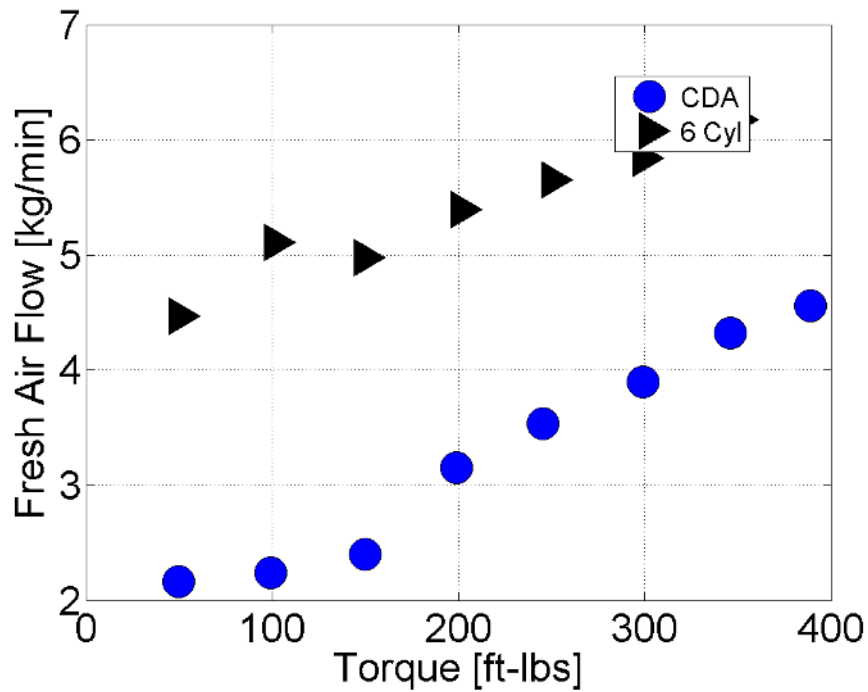


Figure 2.6. Airflow vs. Torque at 1200 RPM in Cylinder Deactivation.

where  $FuelPower_{in}$  is the total fuel power that enters the engine, and  $BrakePower_{out}$  is the power produced by the engine at the crankshaft. Fig. 2.7 shows the changes in BTE across the same load sweep. At lower loads, there is an improvement in BTE, but at higher loads, BTE during CDA actually decreases the efficiency of the engine. To further examine why a dichotomy between low and high loads exists, additional efficiencies are defined. BTE can be decomposed into open cycle, OCE, closed cycle, CCE, and mechanical efficiency, ME, shown as,

$$BTE = OCE * CCE * ME. \quad (2.7)$$

To define OCE, CCE, and ME, several mean effective pressures, MEP, must be defined. MEP is a normalized measure of work done by the engine, and can be used to define work done during different portions of the 4 stroke cycle. Gross indicated mean effective pressure, GIMEP, is the work done by the piston during only the compression and expansion strokes. This work directly captures the engine's ability to convert the

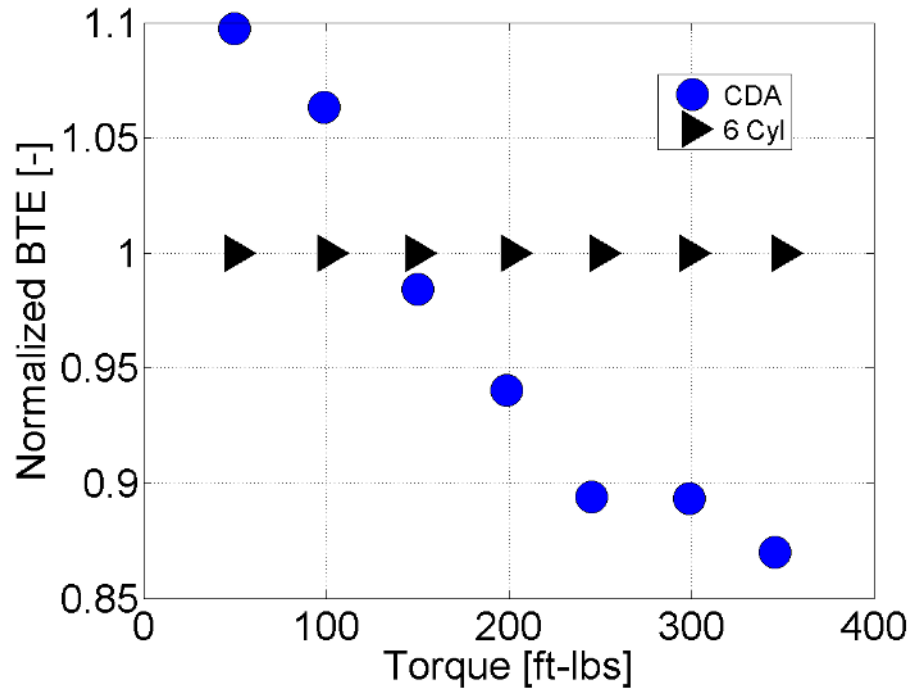


Figure 2.7. Normalized Brake Thermal Efficiency at 1200 RPM in Cylinder Deactivation.

chemical energy of the fuel into mechanical energy seen by the crankshaft. Fig. 2.8 shows the area of the logP-logV diagram which corresponds to GIMEP. Fig.2.9 shows the area of the logP-logV diagram which corresponds to net indicated mean effective pressure, NIMEP, which is the entire area underneath the logP-logV curve. NIMEP is the work done by the engine during the engine 4 stroke process including the intake, compression, expansion, and exhaust strokes. By including the work done during the intake and exhaust strokes, the work done by the piston on the cylinder charge is captured. This work is often defined as pumping mean effective pressure, PMEP, and is illustrated in Fig.2.10. Two additional MEP's often used in engine performance are brake mean effective pressure, BMEP, and friction mean effective pressure, FMEP. BMEP is the normalized power output from the engine at the crankshaft. FMEP is the friction work done on the engine as the work is transferred from the piston to the

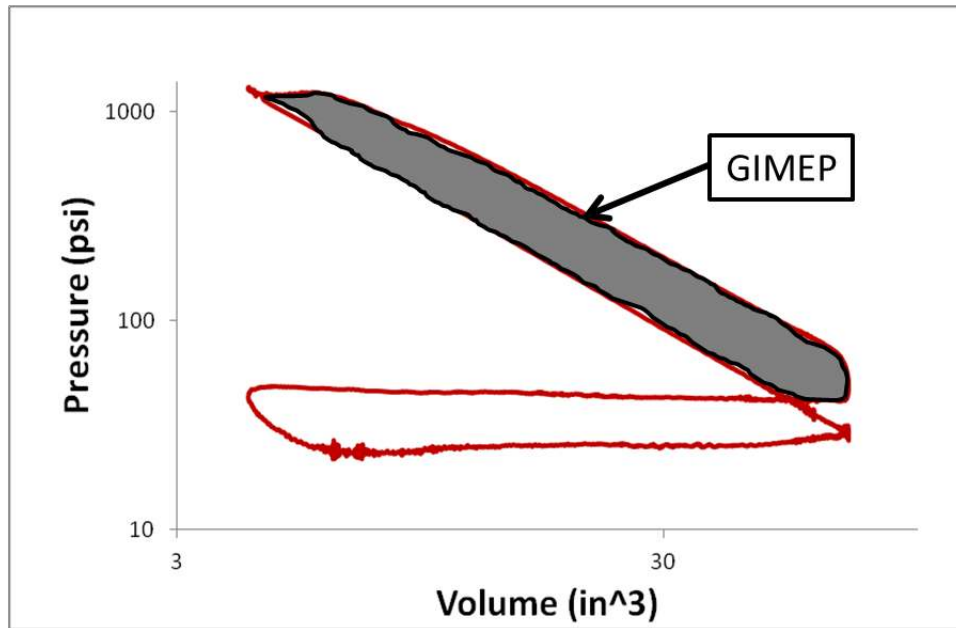


Figure 2.8. LogP-LogV Diagram - Gross Indicated Mean Effective Pressure, GIMEP.

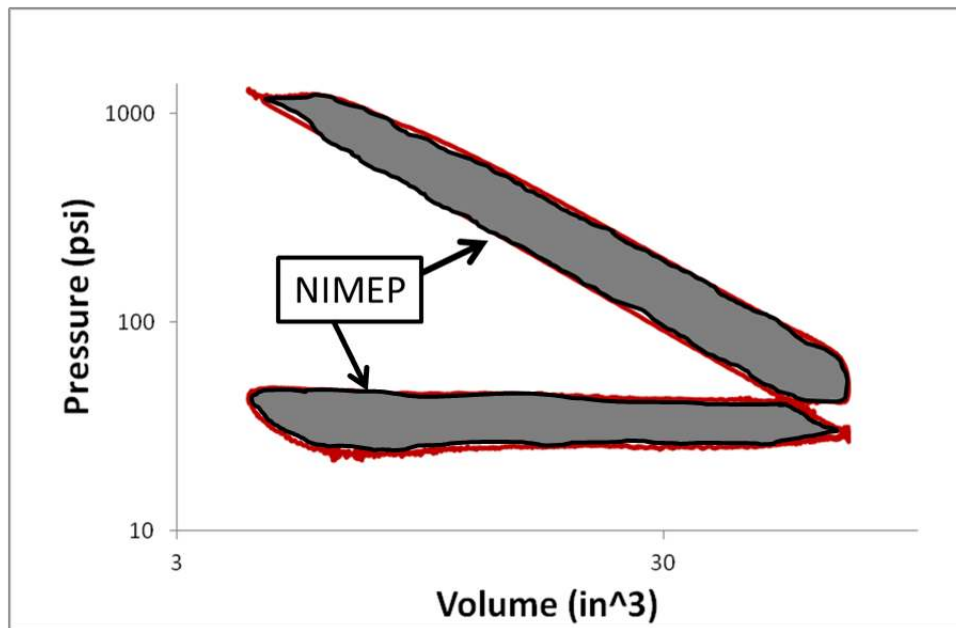


Figure 2.9. LogP-LogV Diagram - Net Indicated Mean Effective Pressure, NIMEP.

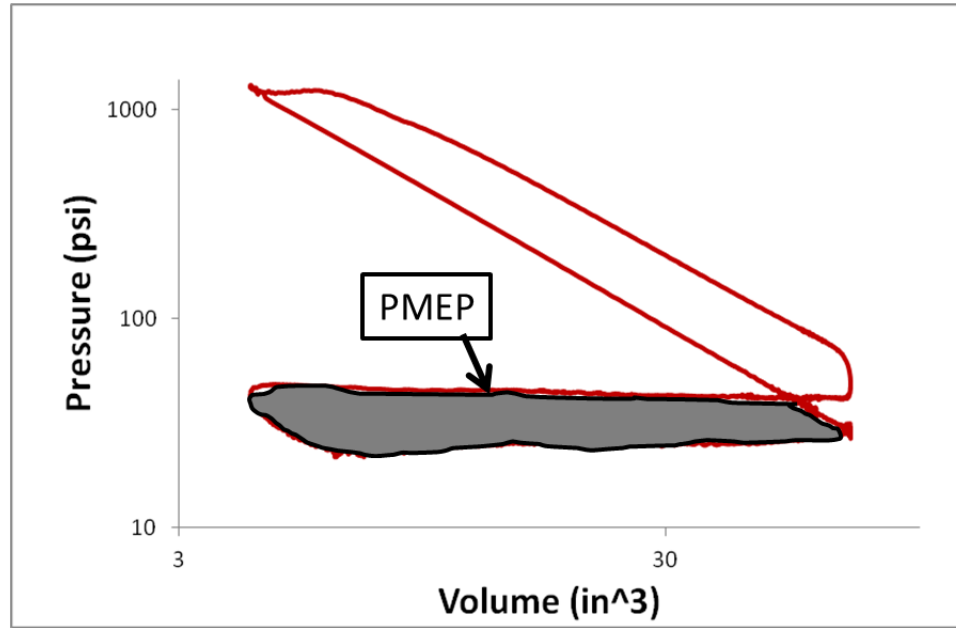


Figure 2.10. LogP-LogV Diagram - Pumping Mean Effective Pressure, PMEP.

crankshaft. FMEP also includes any accessory loads on the engine. As defined in Eq.2.10,

$$OpenCycleEfficiency = \frac{NIMEP}{GIMEP} = \frac{GIMEP - PMEP}{GIMEP}, \quad (2.8)$$

open cycle efficiency, OCE, is the ratio between the net indicated mean effective pressure, NIMEP, and gross indicated mean effective pressure, GIMEP. CCE is defined as the ratio of GIMEP to fuel power which captures the efficiency of converting chemical fuel power into mechanical piston work,

$$ClosedCycleEfficiency = \frac{GIMEP}{FuelPower}. \quad (2.9)$$

Lastly, mechanical efficiency is defined as the ratio between BMEP and engine NIMEP which captures the amount of friction produced in various engine components as well as any accessory loads on the engine,

$$MechanicalEfficiency = \frac{BMEP}{NIMEP} = \frac{NIMEP - FMEP}{NIMEP}. \quad (2.10)$$

Using these definitions, it can be observed that OCE is the measure of the pumping work done by the engine. If the engine does less work to get the charge in and out of

the cylinders, open cycle efficiency will be higher whereas if a large amount of piston work goes into intake and exhaust, OCE will be lower. Fig.2.11 shows that at low loads, OCE is higher in CDA whereas at higher loads it is comparable with 6 cylinder operation. The decrease in OCE at high loads can be attributed to raising  $P_{im}$  in order to drive the required airflow. By raising the pressure across the engine, more pumping work is required as demonstrated in Fig.2.12. The other major component

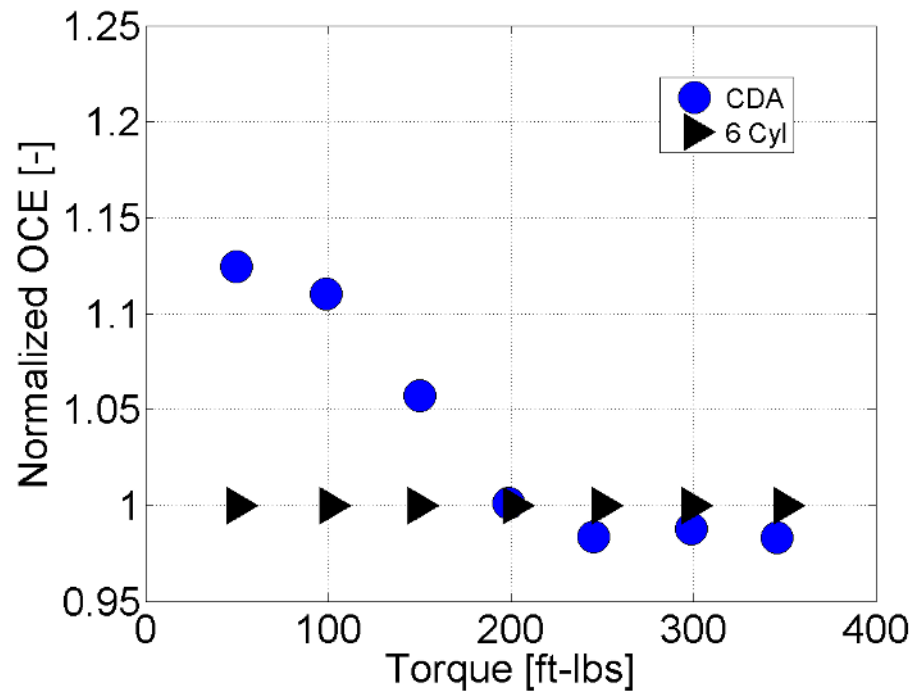


Figure 2.11. Normalized Open Cycle Efficiency at 1200 RPM in Cylinder Deactivation.

of BTE, CCE can determine the effectiveness of fuel combustion. Fig.2.13 shows the comparison of CCE, and it can be observed that at low loads, the CCE in CDA is slightly better than 6 cylinder operation, but becomes much worse as load increases. One of the primary drivers in the CCE decrease is the late main injection timings shown in Fig.2.14. As the load gets higher, later and later injections are used to keep BSNO<sub>x</sub> emissions within reason. Since no EGR is used, the most effective way to maintain BSNO<sub>x</sub> emissions is to push injection timings farther and farther after TDC.

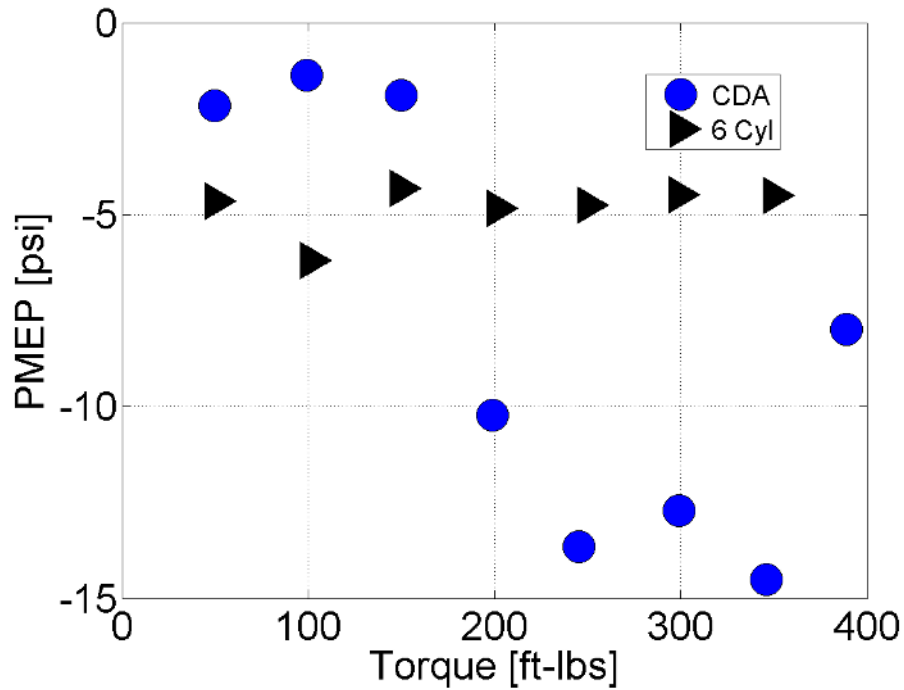


Figure 2.12. PMEP at 1200 RPM in Cylinder Deactivation.

Additionally, the increase in cylinder temperatures promotes more heat transfer from the cylinder taking away from the piston work during expansion.

To summarize, at 1200RPM, the maximum achievable load in CDA was 390 ft-lbs and limited by turbine inlet temperature constraints. CDA was effective in significantly raising TOT across the load range as a result of decreased AFR caused by the reduction in engine displacement. When compared to 6 cylinder operation, BTE is improved at lower loads but does not offer any efficiency gains at moderate and high loads. The primary driver in BTE improvement at low loads is improved open cycle efficiency performance since the improvement in CCE between 3 and 6 cylinder is small. At high loads, OCE is lowered in an effort to drive sufficient airflow through the engine, and CCE is penalized by late SOI timings and heat transfer.



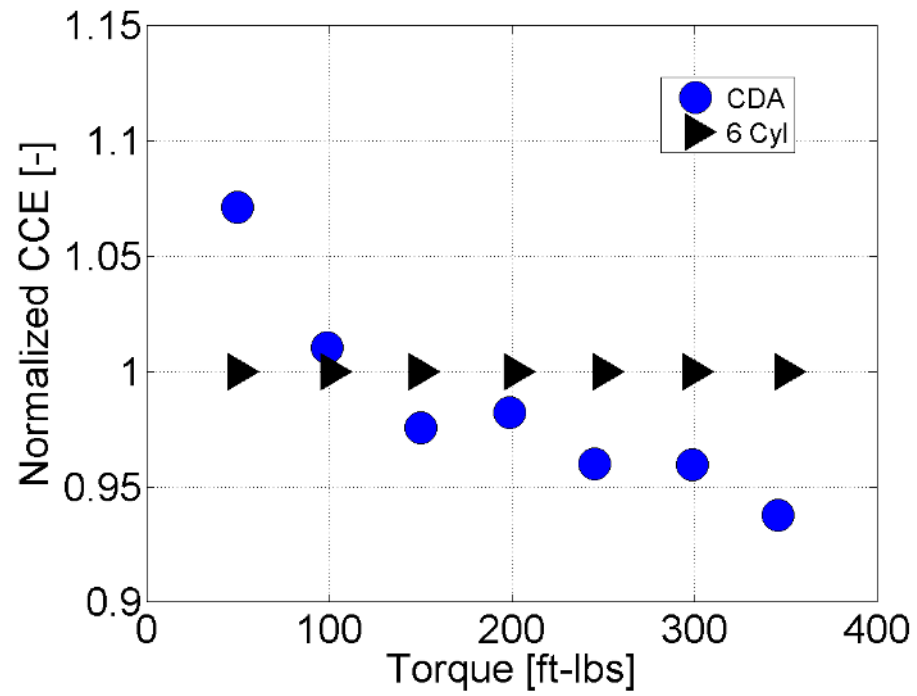


Figure 2.13. Normalized Closed Cycle Efficiency at 1200 RPM in Cylinder Deactivation.

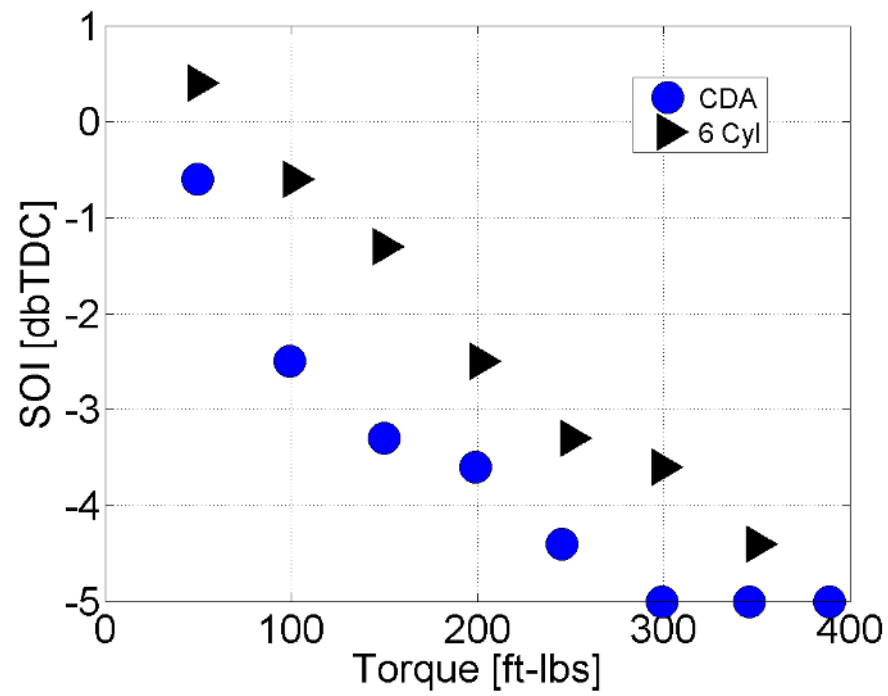


Figure 2.14. Main Injection Timing at 1200 RPM in Cylinder Deactivation.

### 3. EFFECT OF CYLINDER DEACTIVATION AND LATE INTAKE VALVE CLOSING ON EXHAUST GAS TEMPERATURES

While CDA proved to be effective at increasing exhaust gas temperatures across a load sweep at 1200RPM by reducing the air to fuel ratio, at lower loads, there is still some AFR margin available that could be used to further increase turbine outlet temperatures. To further reduce AFR, late intake valve closing, LIVC can be used in conjunction with CDA to reduce air flow through the engine. This combination could increase exhaust gas temperatures to the desired 250°C threshold even at extremely low load conditions where standard 6 cylinder operation produces very low temperatures.

#### 3.1 Effect of Opening VGT on AFR

One of the first ways further AFR reduction can be gained after entering CDA is to simply open the VGT which will decrease the intake manifold pressure. From the speed density equation,

$$W_{air} = \frac{\eta_v P_{im} V_d N}{n R T_{im}}, \quad (3.1)$$

the reduction in  $P_{im}$  will drive less air into the cylinder. Depending on the initial starting position of the VGT, the method can cause a significant reduction in AFR, and at higher loads, it is necessary to keep the VGT squeezed in order to run at those conditions.

#### 3.2 Effect of Cylinder Deactivation and LIVC on AFR

Like CDA, the LIVC affects AFR by reducing the airflow through the engine; however, where cylinder deactivation accomplishes this by reducing the displacement

of the engine, LIVC directly affects the volumetric efficiency of the engine. By closing the intake valve late, some of the charge originally inducted into the cylinder is pushed back out into the intake manifold reducing the amount of charge trapped. In the case of no EGR, the amount of air trapped in cylinder is reduced which reduces the air to fuel ratio.

The effect of late and early intake valve closing on volumetric efficiency can be captured by sweeping IVC from the nominal timing of 565 CAD. The results of such a sweep in 6 cylinder operation is shown in Fig. 3.1. With the VVA system installed on the engine, IVC timing can be delayed up to 675 CAD which will reduce the volumetric efficiency from 0.92 to approximately 0.70. As with CDA, the effect of

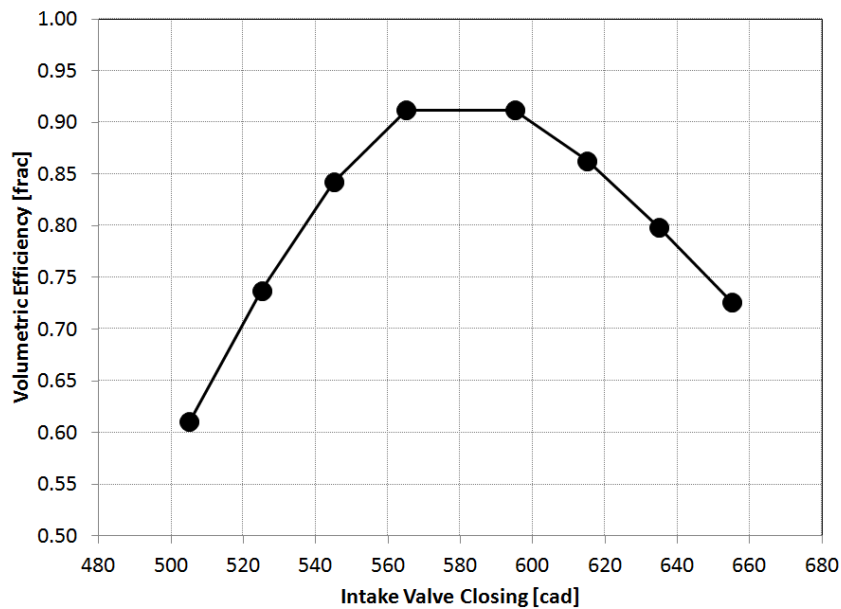


Figure 3.1. Volumetric Efficiency vs. Intake Valve Close Timing.

reducing volumetric efficiency can be captured by the speed density equation. Much like the reduction in engine displacement, the reduction in volumetric efficiency causes a proportional decrease in engine airflow.

One of the major differences between reducing AFR through CDA or LIVC is the tunable nature of LIVC whereas CDA is a binary on-off system. In this study,

Table 3.1. Load Sweeps Performed.

Sweep Number	Conditions
1 <sup>st</sup> Sweep	CDA+Open VGT
1 <sup>st</sup> Sweep	CDA+Open VGT+LIVC625
1 <sup>st</sup> Sweep	CDA+Open VGT+LIVC645
1 <sup>st</sup> Sweep	CDA+Open VGT+LIVC655
1 <sup>st</sup> Sweep	CDA+Open VGT+LIVC675

cylinder deactivation is either 3 or 6 cylinders so the overall displacement is either 6.7L or 3.35L, but LIVC can be as small as 1 degree late or 110 degrees late. By combining these two functions, a greater degree of flexibility is gained in modulating exhaust gas temperatures.

To examine the effect of different CDA and LIVC timings, several load sweeps were conducted, and are outlined in Table 3.1. Beginning with the previous sweep with only CDA, at each load where AFR could be lowered, the VGT was maximally opened. If the AFR could be further reduced, IVC timing was increased to 625 CAD, and this process was repeated until the maximal timing of 675 CAD was achieved.

### 3.2.1 Exhaust Temperature Effects

Fig. 3.2 shows the results from the sweeps described. Up to 250ft-lbs, the VGT could be opened up to decrease AFR although, as seen in Fig. 3.3, this only provided a slight decrease in AFR as the VGT was fairly open to start, although the small change produced significant increases in TOT at higher loads. Above 250ft-lbs, the VGT needed to remain closed in order to run at the higher loads. IVC can be increased to 625 CAD up to 200 ft-lbs, 645 CAD up to 150 ft-lbs, 655 CAD up to 100 ft-lbs, and at 50 ft-lbs, the maximum timing of 675 CAD could be used. In each case, advancing LIVC later and later reduces AFR further and further increasing TOT. At 50-ftlbs, the latest LIVC timing can be used in combination with CDA to increase TOT from 150°C to 250°C demonstrating that it is possible to raise TOT up to the

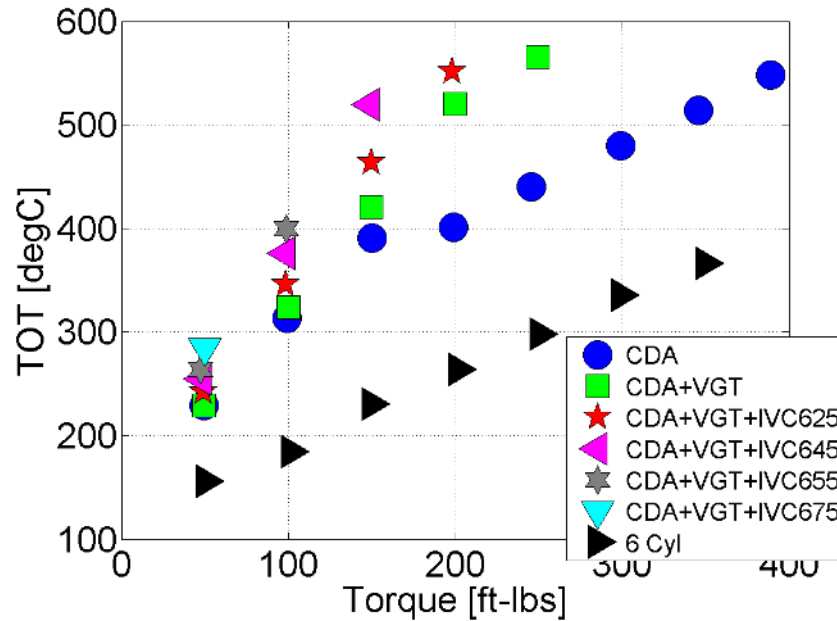


Figure 3.2. Turbine Outlet Temperature vs. Torque at 1200 RPM in Cylinder Deactivation and LIVC.

desired limit even at the lowest baseline TOT. As discussed previously, the reduction in AFR is a result of reduced airflow through the engine as shown in Fig. 3.4. Opening the VGT has the most significant effect at higher loads where the VGT was more closed than at lower loads. At lower loads, LIVC reduces airflow further as timing progresses by reducing the volumetric efficiency. As discussed in Eq. 5.2, this decrease in volumetric efficiency decreases the airflow through the engine. Fig. 3.5 shows the volumetric efficiency for each sweep, and the volumetric efficiency in cylinder deactivation is based on the three active cylinders. Cylinder deactivation improves volumetric efficiency over 6 cylinder operation, but when LIVC is introduced, the volumetric efficiency can be decreased as far as approximately 0.80 at the latest timing.

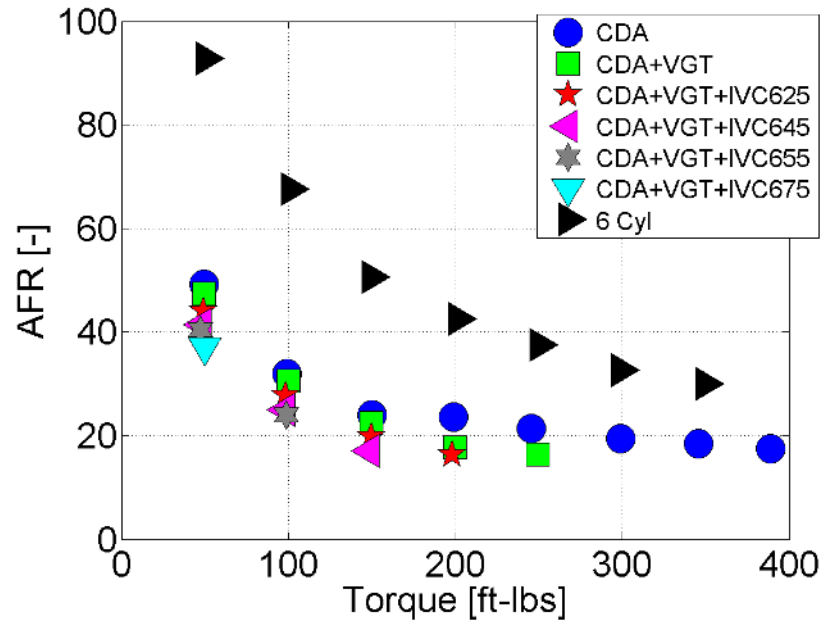


Figure 3.3. Air to Fuel Ratio vs. Torque at 1200 RPM in Cylinder Deactivation and LIVC.

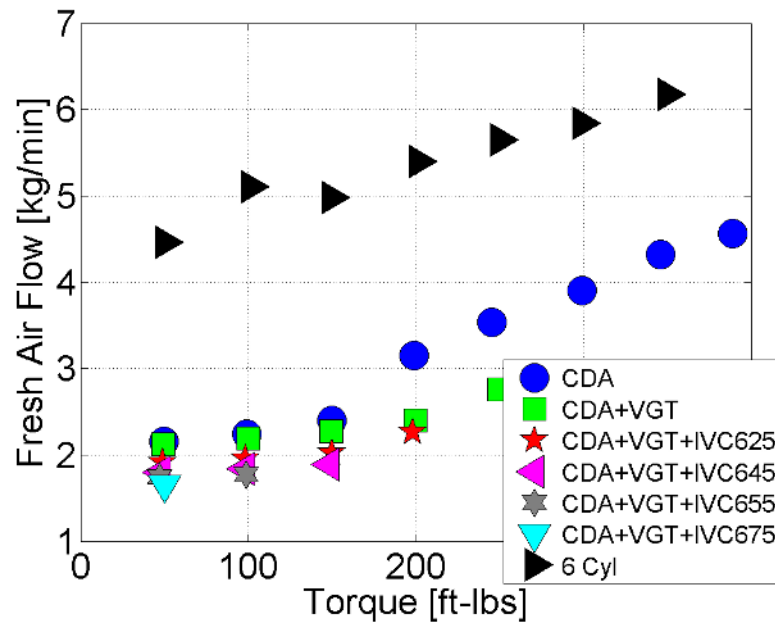


Figure 3.4. AirFlow vs. Torque at 1200 RPM in Cylinder Deactivation and LIVC.

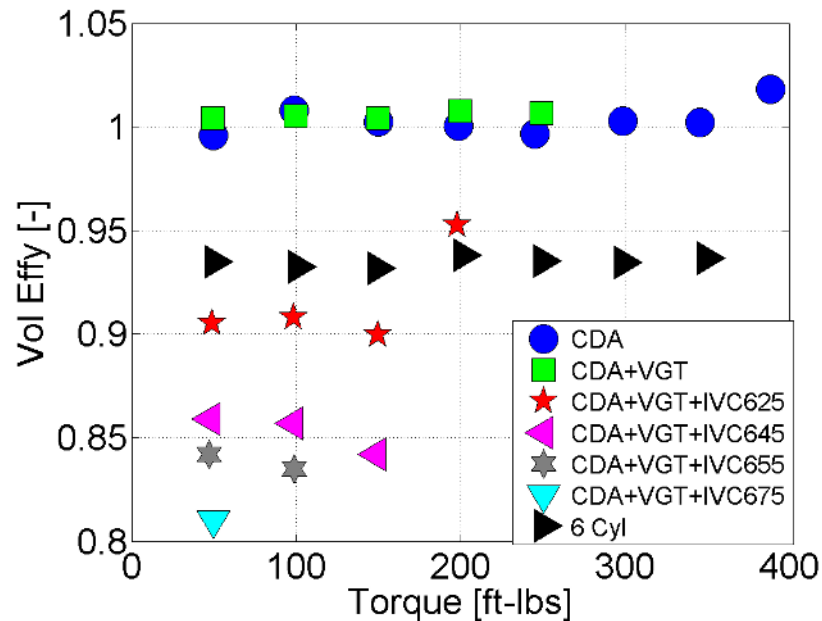


Figure 3.5. Volumetric Efficiency vs. Torque at 1200 RPM in Cylinder Deactivation and LIVC.

### 3.2.2 Engine Performance Effects

As shown in Chapter 2, at low load cases, the reduction in airflow through the engine can improve the engine's ability to "breathe", and improve BTE. Therefore, it would be expected that with the introduction of LIVC at low loads, the engine efficiency could be improved even further. However, as shown in Fig. 3.6, LIVC appears to hurt engine efficiency, and in the case of 100 ft-lbs, even bring efficiency back to 6 cylinder levels. To determine the factors behind this drop off, a similar analysis is performed examining open and closed cycle efficiency. Fig.3.7 shows the open cycle efficiency for each sweep versus torque, and it can be observed that as LIVC timing is increased, the open cycle efficiency decreases somewhat unexpectedly. By examining the pumping work versus torque as in Fig.3.8, it can be seen that in cylinder deactivation and with an open VGT, the pumping work is extremely low to begin with, and changing LIVC timing only has a moderate effect on pumping. This can also be seen in a plot of intake manifold pressure as in Fig.3.9. At lower loads IMP is relatively



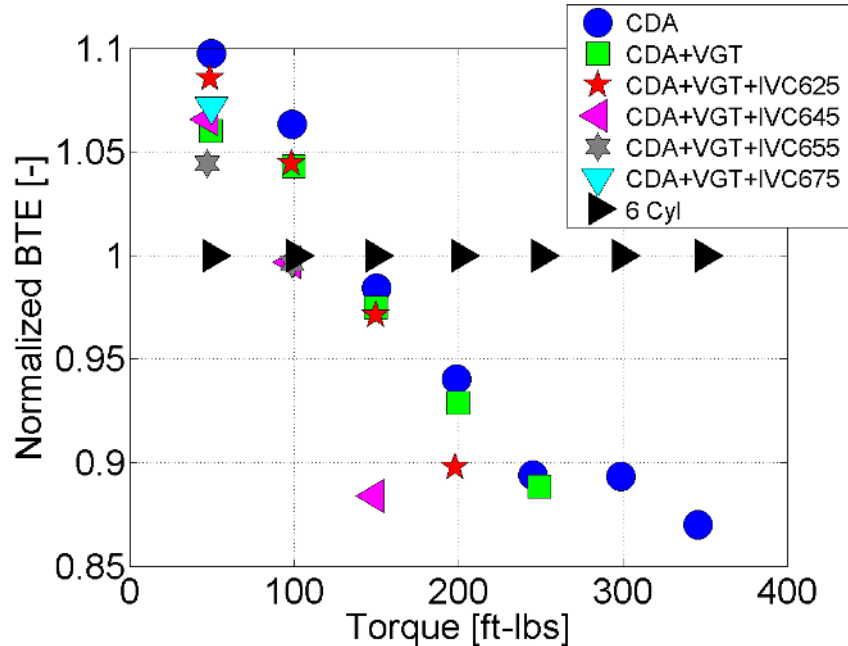


Figure 3.6. Normalized BTE vs. Torque at 1200 RPM in Cylinder Deactivation and LIVC.

close to atmospheric conditions even in 6 cylinder operation, and once the engine enters CDA, IMP drops even farther almost to atmospheric. Therefore, when LIVC is introduced, it has an extremely muted effect on IMP which is seen in the little change in pumping work. So while LIVC reduces the charge trapped in the cylinders thereby reducing airflow, it does not have a significant effect on IMP which takes away any OCE improvement. Fig. 3.10 shows closed cycle efficiency versus torque and shows that at lower loads, LIVC makes only small changes in CCE. However, at higher loads, CCE is drastically reduced as LIVC is pushed later and later. The primary driver of this reduction is a reduced effective compression ratio, ECR, caused by LIVC timing as shown in Fig.3.11. At the latest timing, ECR is as low as 13.5:1 at 50 ft-lbs, and at 150 ft-lbs, ECR is decreased to approximately 16:1. The reduction in compression ratio decreases the overall pressure and temperature inside the cylinder which reduces combustion efficiency directly resulting in a decreased closed cycle efficiency. While BSNO<sub>x</sub> was not the primary focus of the CDA+LIVC study, an interesting trend

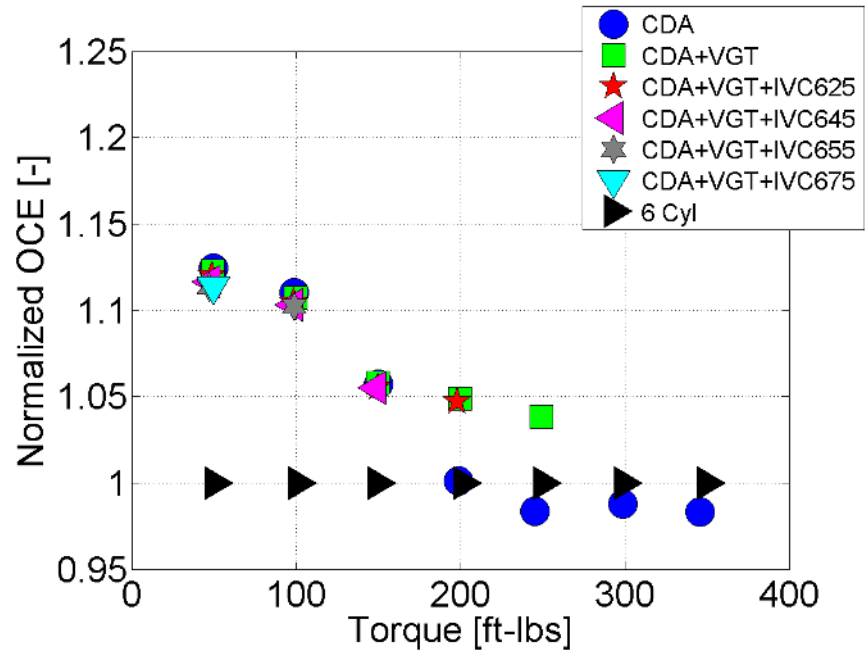


Figure 3.7. Normalized OCE vs. Torque at 1200 RPM in Cylinder Deactivation and LIVC.

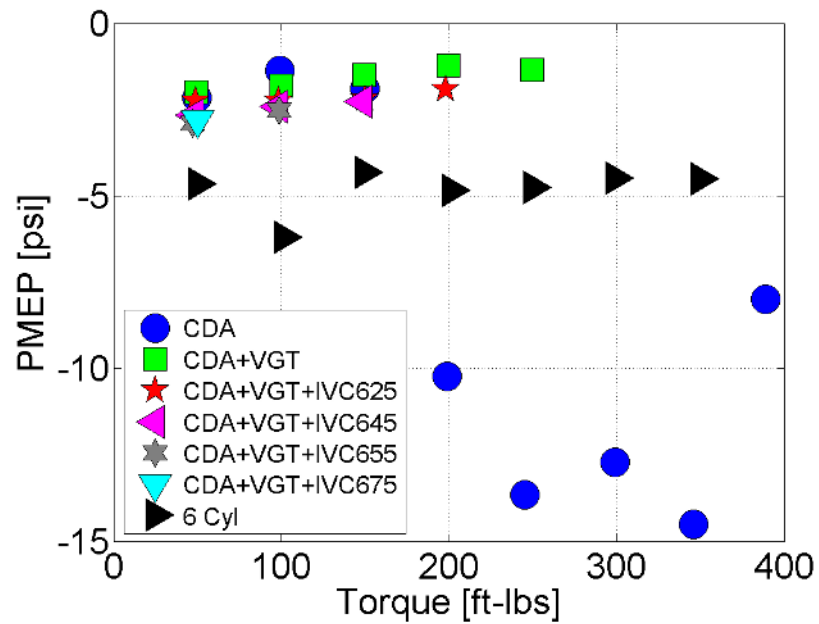


Figure 3.8. PMEP vs. Torque at 1200 RPM in Cylinder Deactivation and LIVC.

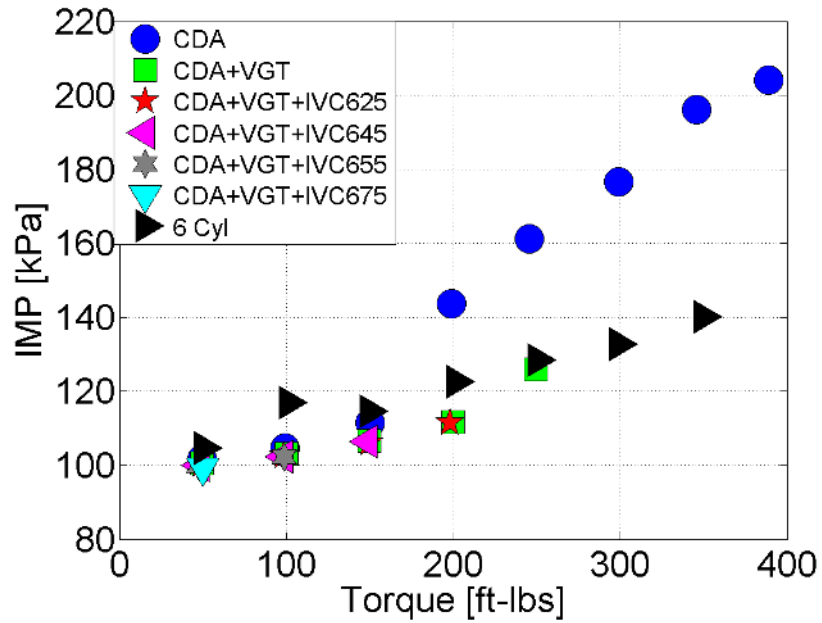


Figure 3.9. IMP vs. Torque at 1200 RPM in Cylinder Deactivation and LIVC.

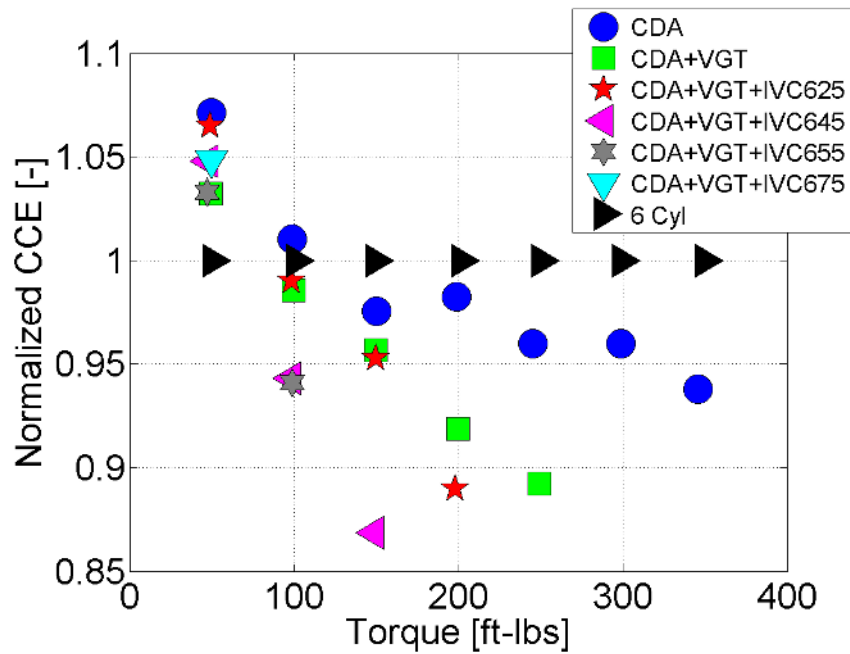


Figure 3.10. Normalized CCE vs. Torque at 1200 RPM in Cylinder Deactivation and LIVC.

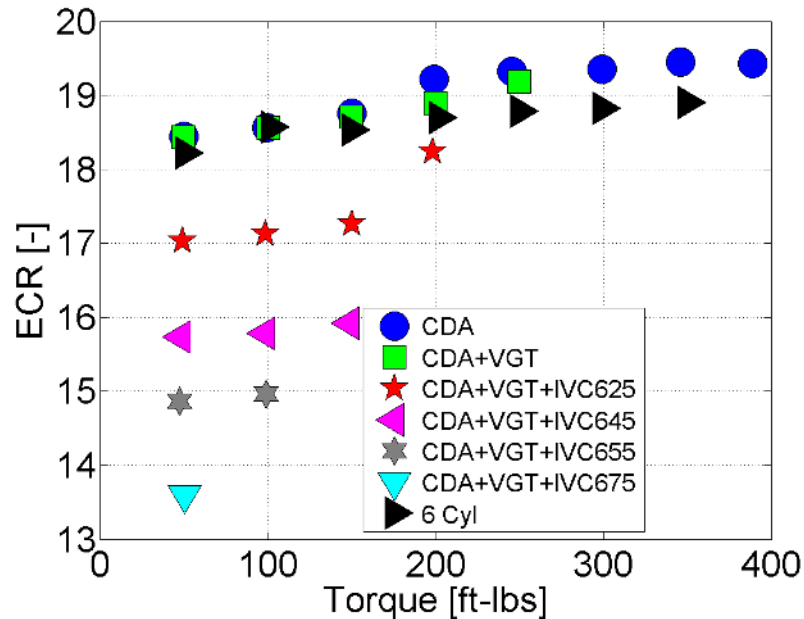


Figure 3.11. ECR vs. Torque at 1200 RPM in Cylinder Deactivation and LIVC.

develops between BSNO<sub>x</sub> and LIVC as shown in Fig.3.12. When LIVC timing is advanced, BSNO<sub>x</sub> emissions decrease at all loads. The BSNO<sub>x</sub> reduction comes from the same reduction in ECR that drove CCE down. The reduction in ECR reduces the peak temperatures during combustion which is one of the primary factors in NO<sub>x</sub> formation. By lowering this temperature, less NO<sub>x</sub> is formed.

To summarize, at 1200RPM, the maximum achievable load in CDA with the addition of LIVC can be increased to 625 CAD up to 200 ft-lbs, 645 CAD up to 150 ft-lbs, 655 CAD up to 100 ft-lbs, and at 50 ft-lbs, the maximum timing of 675 CAD could be used. The higher loads were limited by turbine inlet temperature constraints. LIVC was effective in raising TOT higher across the load range as a result of decreased AFR caused by the reduction in volumetric efficiency. When compared to CDA only operation, BTE does not improve due to a reduction in both open cycle efficiency and close cycle efficiency. LIVC does not provide an improvement in OCE because IMP is almost atmospheric to start so there is almost no margin for PMEP gains. CCE is decreased with LIVC use because of the reduction in ECR reduces combustion

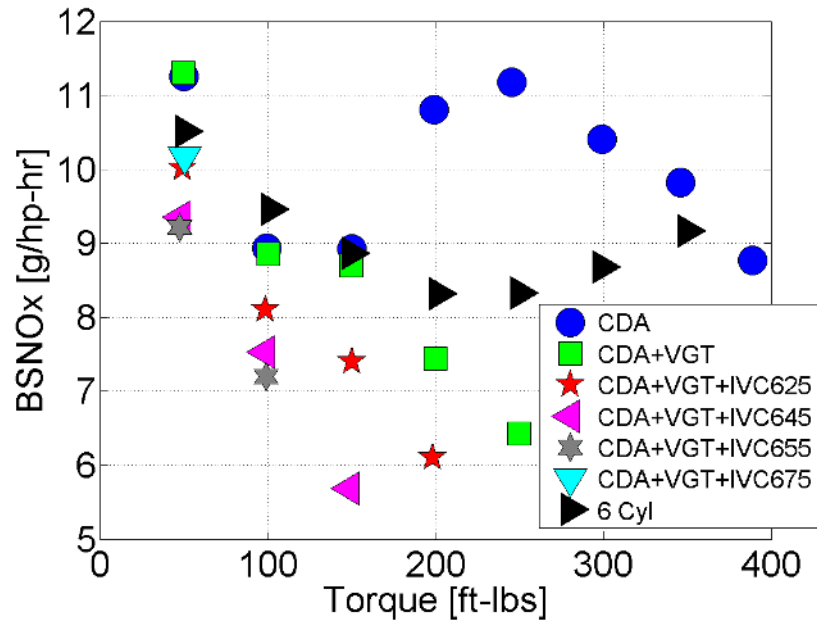


Figure 3.12. BSNOx vs. Torque at 1200 RPM in Cylinder Deactivation and LIVC.

efficiency, but the ECR reduction also results in a reduction in BSNOx emissions. Therefore, CDA+LIVC can improve after treatment performance by simultaneously reducing engine out NOx emissions as well as providing sufficient heat to the after treatment system even at low loads.

#### 4. CYLINDER DEACTIVATION RANGE MEETING NOX EMISSION TARGETS

The previous chapters demonstrated the capability of cylinder deactivation and cylinder deactivation and LIVC to increase TOT to heat up the after treatment systems. Both cases proved successful, and when CDA is solely applied, at low loads, the efficiency of the engine is improved. In the previous studies, control of emissions, specifically BSNO<sub>x</sub>, was not a primary concern; however, to become a commercially viable system, cylinder deactivation must be able to meet BSNO<sub>x</sub> requirements. To investigate the performance of cylinder deactivation while meeting such constraints, three load sweeps as performed in Chapter 2 were performed, but this time a specific BSNO<sub>x</sub> level was targeted across each sweep. The targets were 1.5, 3, and 4 g/hp-hr which represent typical engine out NO<sub>x</sub> emissions from commercially available engines. The main lever used to produce these BSNO<sub>x</sub> levels was exhaust gas recirculation which was not used previously. A similar analysis will be used first examining the ability to increase TOT to heat the after treatment and then examining the effect on engine efficiency.

##### 4.1 Exhaust Temperature Effects

Fig.4.1 shows the results of the sweep conducted, and as previously shown, CDA is successful in raising turbine out temperature. The 6 cylinder baseline to which the results are compared also uses EGR and has BSNO<sub>x</sub> emissions between 3 and 4 g/hp-hr although none of the results presented (3 or 6 cylinder) are optimized results. There is a small amount of variation in TOT at each load between the different BSNO<sub>x</sub> targets. This will be shown to be a result of the different EGR fractions required to meet them. At 1.5 g/hp-hr, the maximum achievable load was approximately 300 ft-lbs. At 3 g/hp-hr, the maximum achievable load was approximately 315 ft-lbs,

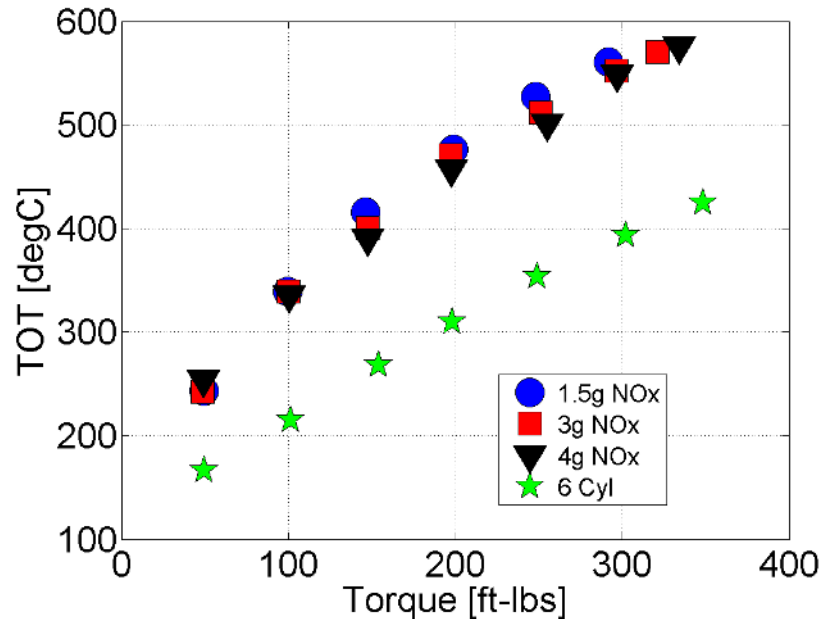


Figure 4.1. TOT vs. Torque at 1200 RPM in Cylinder Deactivation with NOx Targets.

and at 4 g/hp-hr, the maximum achievable load was approximately 325 ft-lbs. As the NOx target is decreased, more EGR is required which decreases AFR (shown in Fig.4.3) increasing TIT (shown in Fig.4.2) which was the limiting factor in all three cases. When EGR is combined with cylinder deactivation, AFR is decreased further because the EGR displaces the air trapped in cylinder so the charge flow stays the same, the airflow decreases (shown in Fig.4.4) leading to lower AFR. This effect is clearly visible in Fig.4.3 at 50 ft-lbs where AFR decreases as the NOx target is lowered corresponding to higher EGR fractions. Above 150 ft-lbs, the AFR is consistently less than twenty which produces minimum turbine outlet temperatures of 400°C at 150 ft-lbs. Even at lower load cases such as 50 ft-lbs, the minimum TOT is approximately 250°C which is the minimum threshold for after treatment heating.

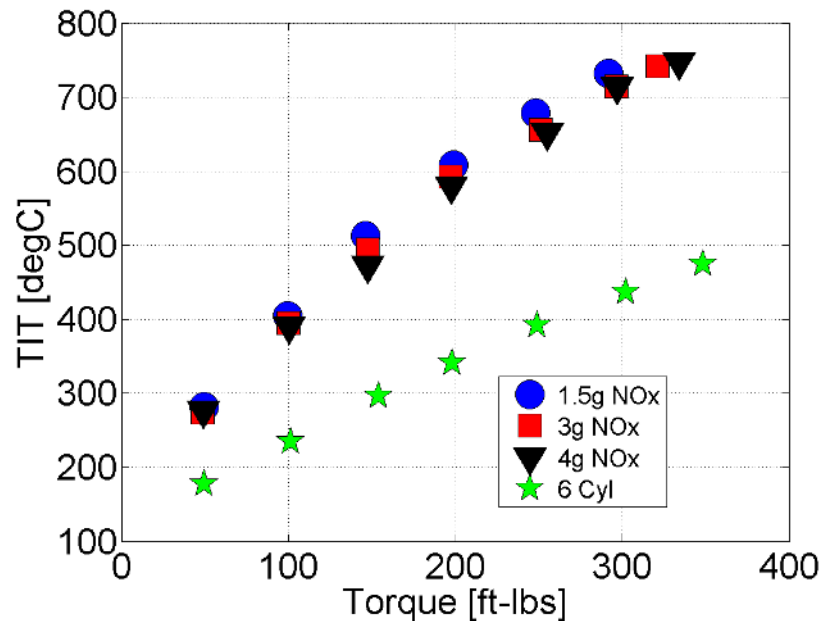


Figure 4.2. TIT vs. Torque at 1200 RPM in Cylinder Deactivation with NOx Targets.

## 4.2 Engine Performance Effects

Examining the effect of meeting NOx targets in Fig.4.5, it can be seen that the previous trends hold when EGR is introduced into engine operation. At 50 ft-lbs, there is an improvement in BTE even as the NOx target gets smaller. However, at high loads, there is a reduction in BTE, and as the NOx target gets smaller, the efficiency gets worse. Fig.4.6 shows that a portion of the BTE improvement at 50 ft-lbs is an improvement in open cycle efficiency. At this low load, the exhaust and intake manifold pressures are both close to atmospheric even with the VGT slightly closed to drive EGR. However, this improvement disappears at high loads where higher EGR fractions are required. To meet the requirements, the VGT is closed to build up exhaust manifold pressure driving EGR flow as shown in Fig.4.7. The closed cycle efficiency of the engine is shown in Fig.4.8, and follows a similar trend as open cycle efficiency. At 50 ft-lbs, there is an improvement in CCE caused by main injection placement in CDA closer to top dead center, TDC, position as shown



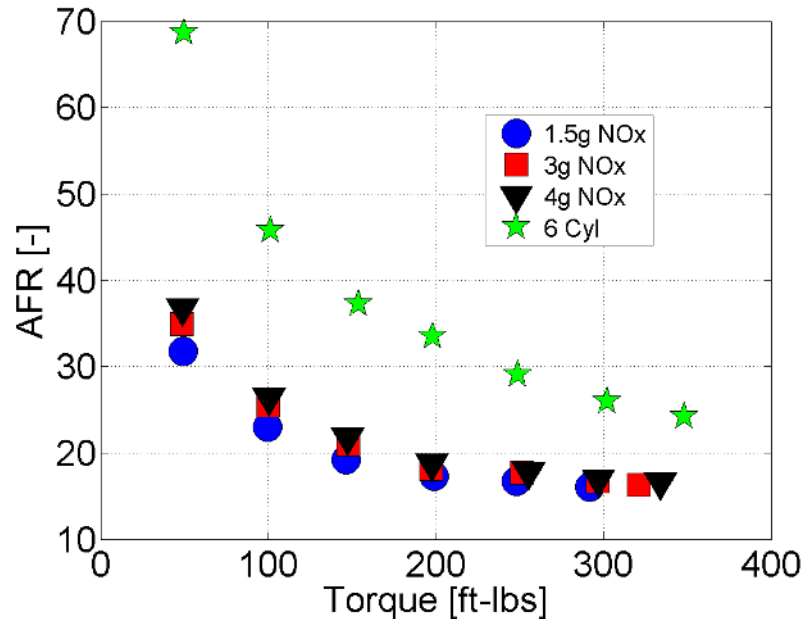


Figure 4.3. AFR vs. Torque at 1200 RPM in Cylinder Deactivation with NOx Targets.

in Fig.4.9. As the centroid of the heat release rate approaches TDC, combustion becomes more efficient combustion improving CCE. From 150 ft-lbs and above, there is a drastic reduction in CCE. This can be attributed to the EGR required, and very late main injection timings that are required at higher loads. EGR reduces combustion efficiency acting as a heat sink during the reaction, and as just described, the extremely late injection timings place the heat release centroid far from TDC reducing CCE. When such high EGR rates are used, especially at higher loads, the AFR can be pushed low enough to create excess soot or PM. As shown in Fig.4.10, at higher loads although the NOx targets are reached, the soot limit of 1.5 FSN is violated or approached. This could make using CDA at higher loads difficult.

To summarize, at 1200RPM, the maximum achievable load in CDA at a NOx target of 1.5 g/hp-hr was 300 ft-lbs, 3 g/hp-hr was 315 ft-lbs, and 4 g/hp-hr was 325 ft-lbs. To meet these NOx requirements, EGR was introduced. The higher loads were limited by turbine inlet temperature constraints. CDA was extremely effective raising

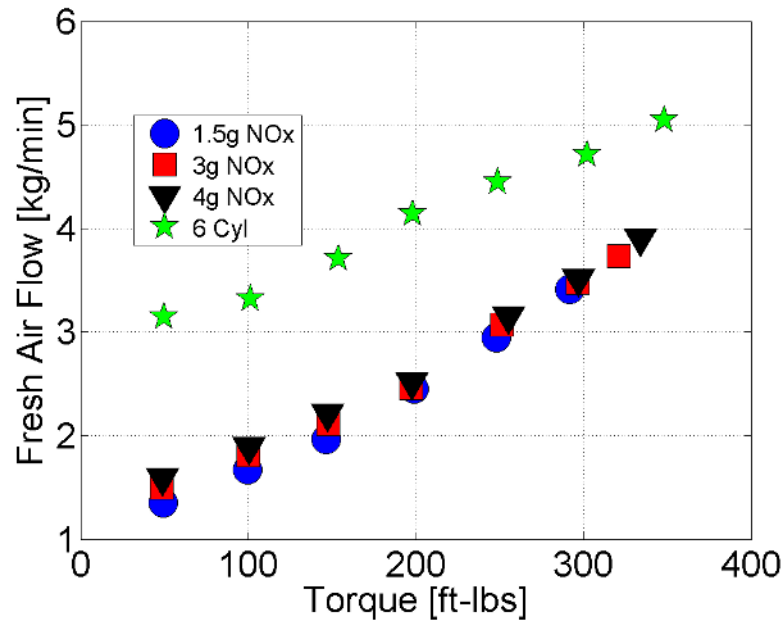


Figure 4.4. Air Flow vs. Torque at 1200 RPM in Cylinder Deactivation with NOx Targets.

TOT higher across the load range as a result of decreased AFR caused the reduction in airflow cause by CDA and the use of EGR. When compared to 6 cylinder operation, BTE improves only at 50 ft-lbs from both improved open cycle efficiency and close cycle efficiency. At higher loads, OCE performance degrades as the VGT must be squeezed maximally to drive sufficient EGR. CCE is reduced due to the combustion efficiency reduction from EGR and late main injection timings used to meet NOx targets. Additionally, at high loads, the high amounts of EGR used increase smoke production. Therefore, when considering relevant NOx targets, CDA can improve after treatment performance up to approximately 300 ft-lbs, but there will be an efficiency penalty above 50 ft-lbs.

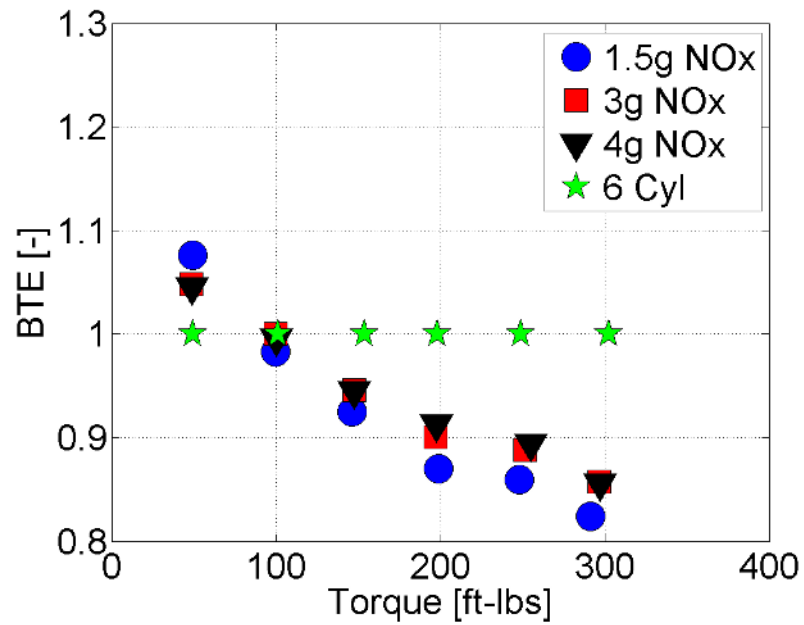


Figure 4.5. Normalized BTE vs. Torque at 1200 RPM in Cylinder Deactivation with NOx Targets.

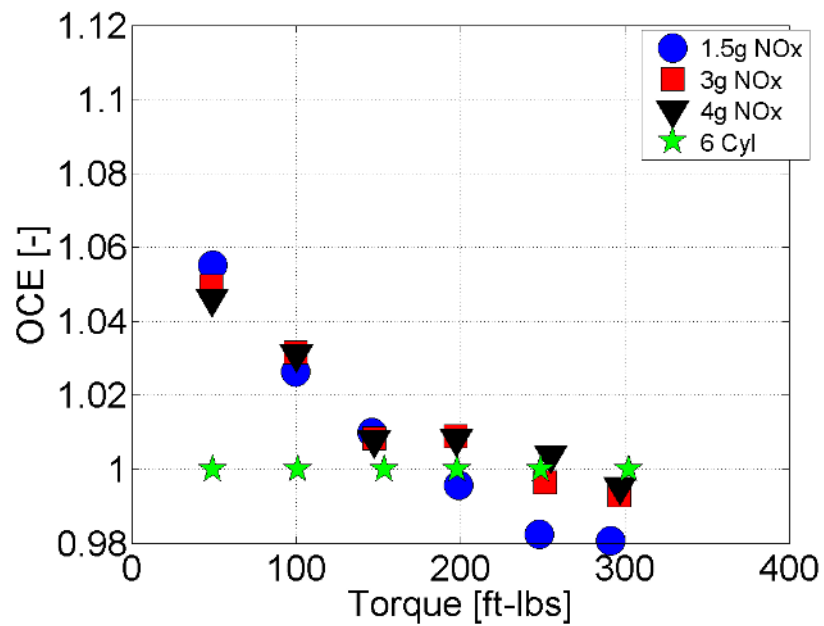


Figure 4.6. Normalized OCE vs. Torque at 1200 RPM in Cylinder Deactivation with NOx Targets.

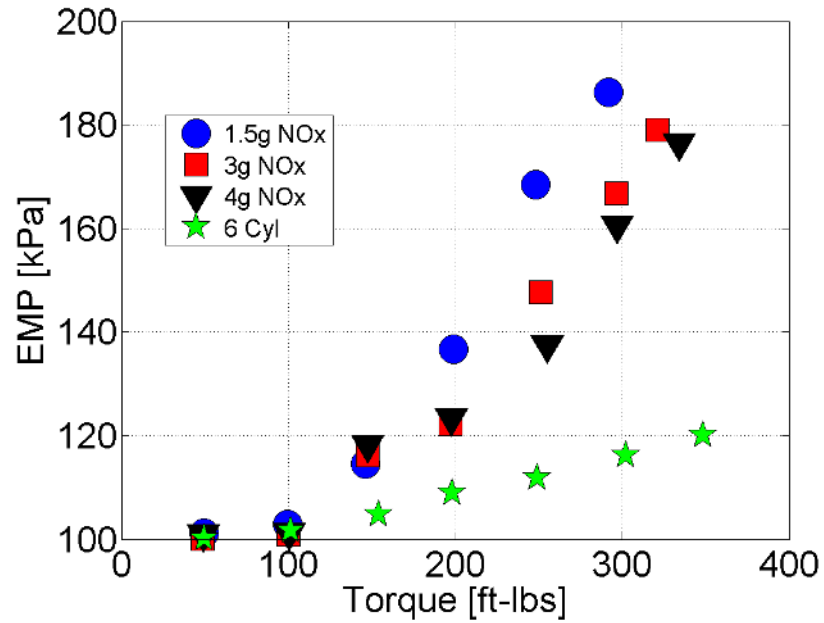


Figure 4.7. EMP vs. Torque at 1200 RPM in Cylinder Deactivation with NOx Targets.

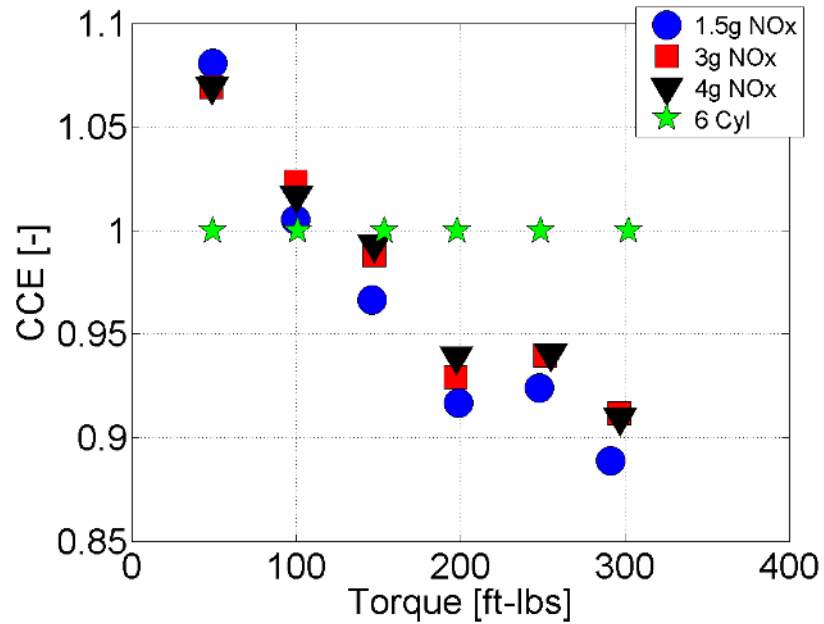


Figure 4.8. Normalized CCE vs. Torque at 1200 RPM in Cylinder Deactivation with NOx Targets.

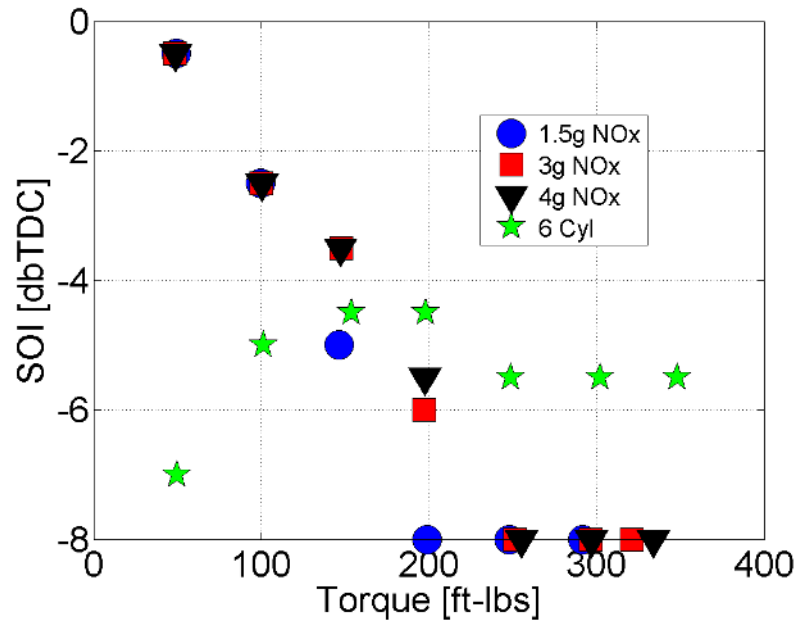


Figure 4.9. SOI vs. Torque at 1200 RPM in Cylinder Deactivation with NOx Targets.

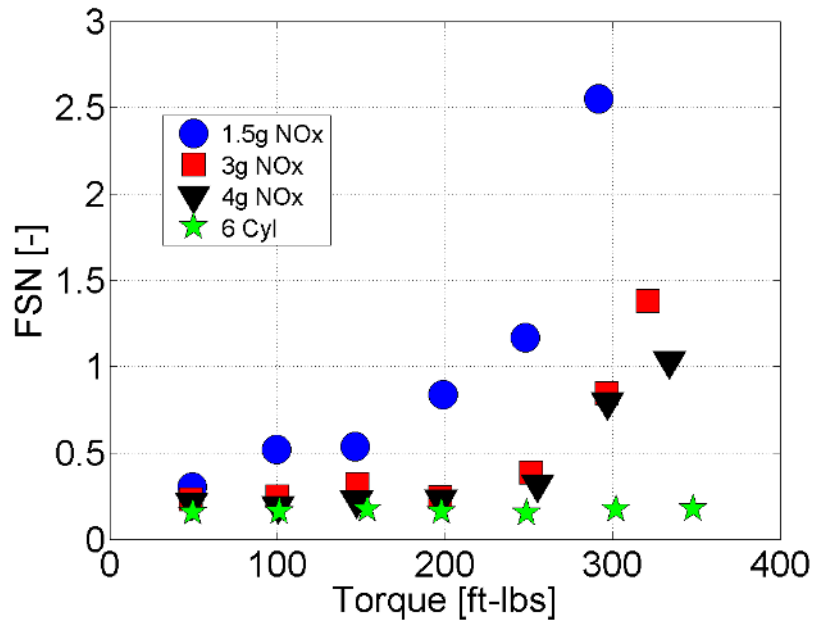


Figure 4.10. FSN vs. Torque at 1200 RPM in Cylinder Deactivation with NOx Targets.

## 5. CONCLUSIONS AND FUTURE WORK

### 5.1 Exhaust Gas Temperature Increase Projection across Operating Map

The previous sweeps have demonstrated the capability of CDA and LIVC to modulate airflow through the engine and decrease AFR, but the focus of this study was only at 1200RPM. To better understand the ability of CDA and LIVC as exhaust thermal management techniques, it is desirable to predict the increased exhaust gas temperatures at all speeds and loads especially at lower loads. Using the relationships previously established between CDA, LIVC, and engine airflow as well as the fit between AFR and TOT, it is possible to create such a projection.

As shown previously, Fig. 5.1 shows the turbine outlet temperature for a stock Cummins ISB engine, and below the black line are the speed and load space where the temperature is below 250°C. This region is where CDA and LIVC could be most effective in raising temperatures as the engine operates in extremely lean conditions as shown by the corresponding air to fuel ratios shown in Fig. 5.2. Using CDA and LIVC to reduce the air flow could enable the engine to operate above 250°C in the whole region. To project the possible increase in TOT, the relationship previously established (shown in Fig. 5.3) between AFR and TOT is used. The outliers below the fitted line are the result of very high EGR fractions, typically those above 30%, and therefore, this projection be skewed in cases where these fractions are used. However, as the plot shows, the outliers only represent a small portion of the engine operating space, which should not adversely effect the TOT increase projections. So if the modified AFR can be determined, then the increase in TOT can be determined as well.

The modified AFR is

$$AFR_{CDA,LIVC} = \frac{AirFlow_{CDA,LIVC}}{FuelFlow}, \quad (5.1)$$

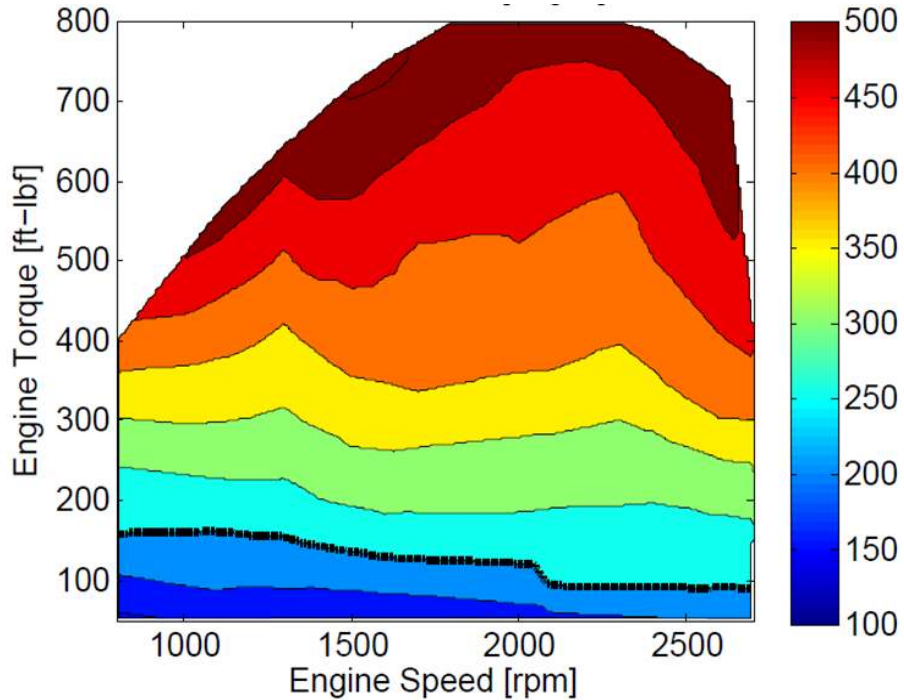


Figure 5.1. Exhaust Gas Temperature for a Cummins 6.7L ISB Engine.

where  $AirFlow_{CDA,LIVC}$  is the modified airflow through the engine and Fuel Flow is the stock fuel flow of the engine. While CDA and LIVC have shown to be capable of modulating engine efficiency and therefore fueling, when compared to the change in airflow, the change in fueling will not have a significant effect on AFR. Therefore, the stock engine fueling is used to calculate AFR. To calculate the decreased airflow through the engine, the speed density equation is again employed,

$$W_{air} = \frac{\eta_v P_{im} V_d N}{n R T_{im}}. \quad (5.2)$$

The first method of decreasing AFR would be to open the variable geometry turbocharger to reduce the intake manifold pressure to atmospheric conditions which can be represented by setting  $P_{im}$  equal to ambient pressure. By deactivating half of the cylinders, CDA will reduce the engine displacement,  $V_d$ , by half. Lastly, at the latest IVC timing, it was observed that the volumetric efficiency,  $\eta_v$ , of the active cylinders was approximately 0.8. With the remaining parameters,  $T_{im}$ , R, and n

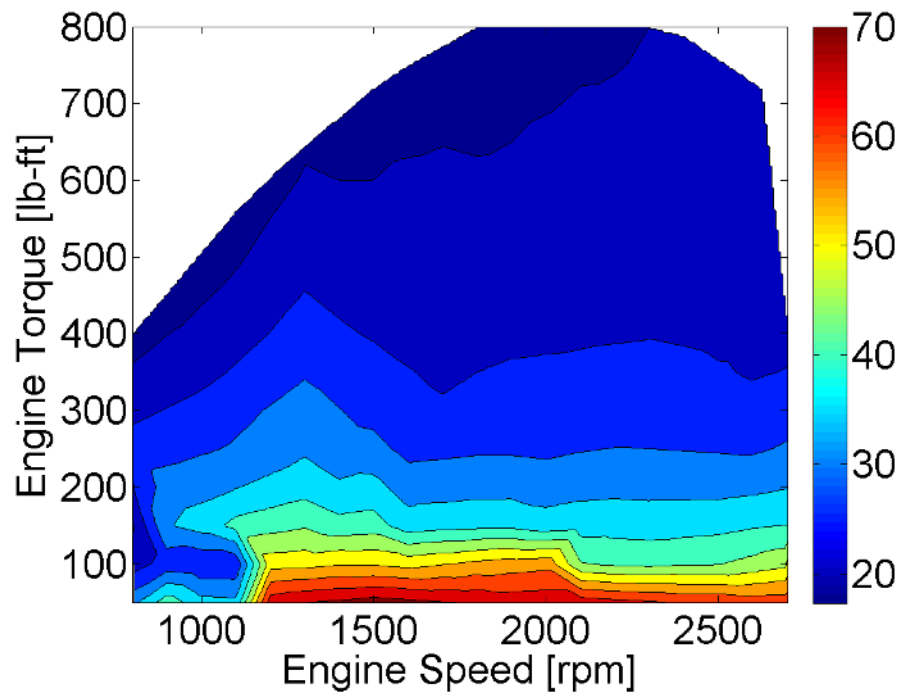


Figure 5.2. AFR for a Cummins 6.7L ISB Engine.

known, the airflow can be calculated and used in the AFR calculation shown above. The resulting TOT is calculated, and the resulting increased turbine outlet temperatures are shown in Fig. 5.4. It can be seen that the entire region that was previously  $250^{\circ}\text{C}$  or less is now well above the limit. This prediction shows that the combination of CDA and LIVC can be used to increase the exhaust temperatures to desirable levels across the operating range of the engine thus proving to be an extremely effective thermal management technique.

However, above 150 to 200ft-lbs, the turbine outlet temperatures are above  $600^{\circ}\text{C}$  which can potentially damage engine components. In these cases, the AFR has been reduced too far and produces undesirable temperature increases. This effect can also be seen in the previous sweeps where air flow had to be increased in order to increase load. These limits could potentially be mitigated by deactivating less cylinders. By deactivating only one or two cylinders at higher loads, the air flow



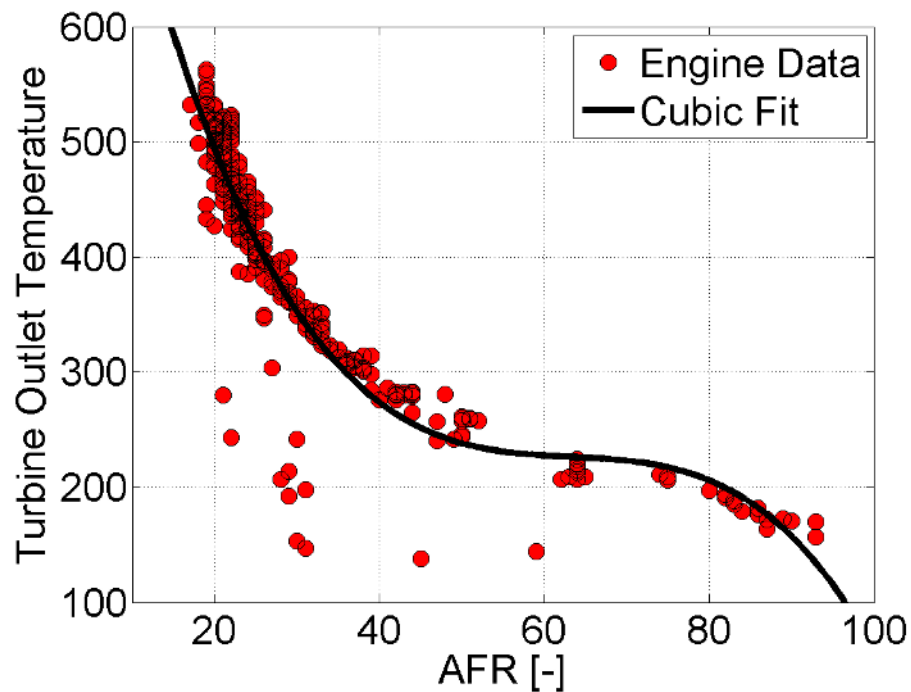


Figure 5.3. Experimental Turbine Outlet Temperature vs. Air to Fuel Ratio.

through the engine could be increased to maintain AFR and avoid the turbine inlet temperature limits. This study only considered deactivation of 3 cylinders, but the range of the thermal efficiency benefits could possibly be extended if other CDA configurations were considered.

## 5.2 Summary and Future Work

Modern aftertreatment systems require high exhaust temperatures to operate efficiently, and low load conditions often do not produce sufficient thermal energy. While many techniques are currently used, modulation of airflow through the engine is one of the most effective. Cylinder deactivation and LIVC can be used to reduce airflow through the engine at levels not achievable with another technology like VGT. The effect of cylinder deactivation and late intake valve closing on the exhaust thermal management and engine performance of a mid size in-line 6 cylinder diesel engine was

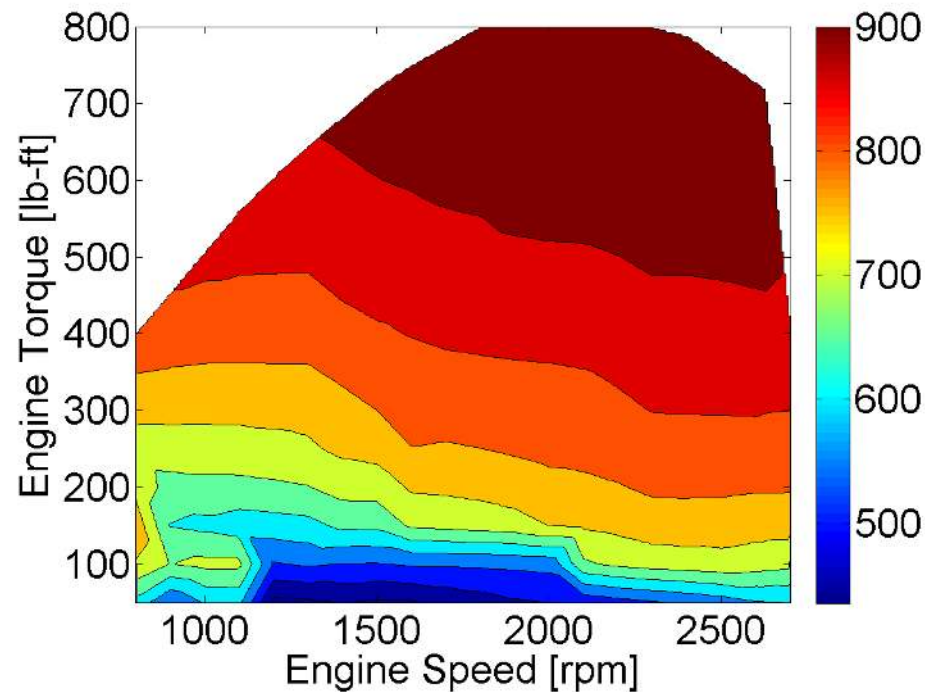


Figure 5.4. Exhaust Gas Temperatures Utilizing CDA and LIVC for a Cummins 6.7L ISB Engine.

examined. In cylinder deactivation operation, cylinders 4,5, and 6 were cut leaving the engine effectively operating as an in line 3. At 1200 RPM, a series of load sweeps were conducted to identify the effects at low and high load conditions. The primary focus of the study was the ability to increase exhaust temperatures, especially at low loads, the maximum achievable loads, and the effect on engine efficiency.

The first set of sweeps only utilized cylinder deactivation without EGR. The maximum achievable load in CDA was 390 ft-lbs and limited by turbine inlet temperature constraints. CDA was effective in significantly raising TOT across the load range as a result of decreased AFR caused by the reduction in engine displacement. When compared to 6 cylinder operation, BTE is improved at lower loads but does not offer any efficiency gains at moderate and high loads. The primary driver in BTE improvement at low loads is improved open cycle efficiency performance since the improvement in CCE between 3 and 6 cylinder is small. At high loads, OCE is lowered in an effort to

drive sufficient airflow through the engine, and CCE is penalized by late SOI timings and heat transfer.

Even with the engine displacement reduced by half, there was still AFR margin up to 200 ft-lbs that could be farther reduced. In each case, the VGT was opened all the way until the intake manifold pressure was almost atmospheric. If there was still AFR margin, intake valve closing time was advanced, reducing the volumetric efficiency of the engine. In CDA, LIVC can be increased to 625 CAD up to 200 ft-lbs, 645 CAD up to 150 ft-lbs, 655 CAD up to 100 ft-lbs, and at 50 ft-lbs, the maximum timing of 675 CAD could be used. The higher loads were limited by turbine inlet temperature constraints. LIVC was effective in raising TOT higher across the load range as a result of decreased AFR caused by the reduction in volumetric efficiency. When compared to CDA only operation, BTE does not improve due to a reduction in both open cycle efficiency and close cycle efficiency. LIVC does not provide an improvement in OCE because IMP is almost atmospheric to start so there is almost no margin for PMEP gains. CCE is decreased with LIVC use because the reduction in ECR reduces combustion efficiency, but the ECR reduction also results in a reduction in BSNO<sub>x</sub> emissions. Therefore, CDA+ LIVC can improve after treatment performance by simultaneously reducing engine out NO<sub>x</sub> emissions as well as providing sufficient heat to the after treatment system even at low loads.

Finally, a series of sweeps were conducted trying to satisfy specific BSNO<sub>x</sub> targets. The maximum achievable load in CDA at a NO<sub>x</sub> target of 1.5 g/hp-hr was 300 ft-lbs, 3 g/hp-hr was 315 ft-lbs, and 4 g/hp-hr was 325 ft-lbs. To meet these NO<sub>x</sub> requirements, EGR was introduced. The higher loads were limited by turbine inlet temperature constraints. CDA was extremely effective raising TOT higher across the load range as a result of decreased AFR due the combined effect of CDA and EGR. When compared to 6 cylinder operation, BTE improves only at 50 ft-lbs from both improved open cycle efficiency and close cycle efficiency. At higher loads, OCE performance degrades as the VGT must be squeezed maximally to drive sufficient EGR. CCE is reduced due to the combustion efficiency reduction from EGR and late main injection timings used

to meet NO<sub>x</sub> targets. Additionally, at high loads, the high amounts of EGR used increase smoke production. Therefore, when considering relevant NO<sub>x</sub> targets, CDA can improve after treatment performance up to approximately 300 ft-lbs, but there will be an efficiency penalty above 50 ft-lbs.

While these results have shown the ability of CDA and LIVC to increase exhaust temperatures and in some cases improve brake thermal efficiency, the sweeps were not optimized results. Further investigation at a given speed and load could improve the results especially efficiency presented previously. At 300 ft-lbs, initial BTE improvement efforts are shown in Fig. 5.5 for both 6 cylinder and 3 cylinder modes in the 1.5 to 4g NO<sub>x</sub> range. It can be seen that some small changes in engine inputs can

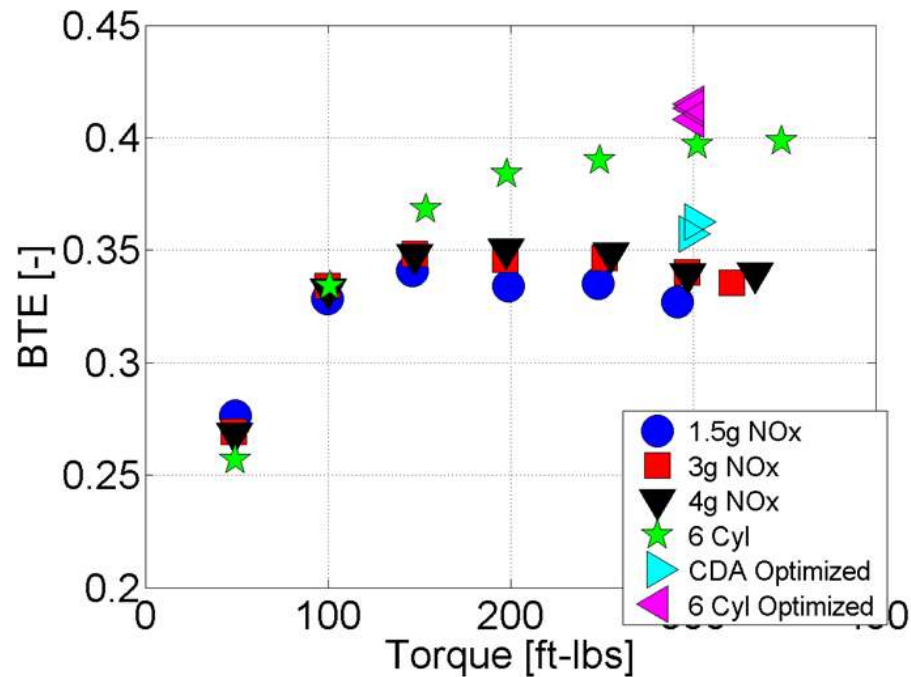


Figure 5.5. Improved BTE vs. Torque at 1200 RPM in Cylinder Deactivation with NO<sub>x</sub> Targets.

improve engine performance in both cases. However, even with some optimization, at 300 ft-lbs, BTE still cannot be improved. In addition, particulate matter and hydrocarbon emissions, resulting from the low AFR, are significantly higher which is also

undesirable. As stated previously, at these high loads deactivation only one or two cylinders maybe more effective than deactivating three as done here. Further studies should include investigation of cylinder deactivation of one, two, and three cylinders at different speeds and loads. This investigation would help establish an operating map where CDA and LIVC could be used for improving thermal management and efficiency. With such a map created, transient operation with CDA and LIVC should be investigated including transition in and out of different operating modes.

## LIST OF REFERENCES

## LIST OF REFERENCES

- [1] Worldwide emissions regulations, 2011.  
[http://cumminsemissionsolutions.com/CES/CESContent//SiteContent/en/Binary\\_Asset/Mature\\_Emissions\\_Evolution\\_Chart.jpg](http://cumminsemissionsolutions.com/CES/CESContent//SiteContent/en/Binary_Asset/Mature_Emissions_Evolution_Chart.jpg).
- [2] W. Addy Majewski. Diesel particulate filters, 2011.  
<http://www.dieselnets.com/tech/dpf.php>.
- [3] W. Addy Majewski. Diesel oxidation catalyst, 2011.  
[http://www.dieselnets.com/tech/cat\\_doc.php](http://www.dieselnets.com/tech/cat_doc.php).
- [4] W. Addy Majewski. Selective catalytic reduction, 2011.  
[http://www.dieselnets.com/tech/cat\\_scr.php](http://www.dieselnets.com/tech/cat_scr.php).
- [5] Ralph McGill Magdi Khair Christine Lambert, Robert Hammerle and Christopher Sharp. Technical advantages of urea scr for light-duty and heavy-duty diesel vehicle applications. *SAE 2004-01-1292*, 2004.
- [6] Matthias Bouchez and Jean Baptiste Dementhon. Strategies for the control of particulate trap regeneration. *SAE 2001-01-0472*, 2001.
- [7] Mike Kass Jim Parks, Shean Huff and John Storey. Characterization of in-cylinder techniques for thermal management of diesel aftertreatment. *SAE 2007-01-3997*, 2007.
- [8] Jeffery D. Naber John H. Johnson Paramjot Singh, Abishek M. Thalagavara and Susan T. Bagley. An experimental study of active regeneration of an advanced catalyzed particulate filter by diesel fuel injection upstream of an oxidation catalyst. *SAE 2006-01-0879*, 2006.
- [9] Eugene Gonze Charles Solbrig Chang Hwan Kim, Michael Paratore and Stuart Smith. Electrically heated catalysts for cold-start emissions in diesel aftertreatment. *SAE 2012-01-1092*, 2012.
- [10] Axel Schatz Ulrich Pfahl and Roman Konieczny. Advanced exhaust gas thermal management for lowest tailpipe emissions - combining low emission engine and electrically heated catalyst. *SAE 2012-01-1090*, 2012.
- [11] Haruyuki Yokota Takaharu Shimizu Hiroyuki Ninomiya Toshiya Akiyoshi, Hisaki Torisaka and Hironori Narita. Development of efficient urea-scr systems for epa 2010 - compliant medium duty diesel vehicles. *SAE 2011-01-1309*, 2011.
- [12] Enrico Corti Davide Moro Matteo De Cesare Nicolo Cavina, Giorgio Mancini and Federico Stola. Thermal management strategies for scr after treatment systems. *SAE 2013-24-0153*, 2013.

- [13] Thorsten Schnorbus Christopher Severin Andreas F. Kolbeck Sharareh Honardar, Hartwig Busch and Thomas Korfer. Exhaust temperature management for diesel engines assessment of engine concepts and calibration strategies with regard to fuel penalty. *SAE 2011-24-0176*, 2011.
- [14] Chr. Lammle M. Wyser A. Mayer, Th. Lutz and F. Legerer. Engine intake throttling for active regeneration of diesel particle filters. *SAE 2003-01-0381*, 2003.
- [15] Q. Lu Y. Huang. Thermal management of a four-way catalyst system with alternative combustions for achieving future emissions standard. *SAE 2007-24-0103*, 2007.
- [16] Peter Eilts Alexander Rempel Sebastian Gehrke, David Kovacs and Peter Eckert. Investigation of vva-based exhaust management strategies by means of a hd single cylinder research engine and rapid prototyping systems. *SAE 2013-01-0587*, 2013.
- [17] T.G. Leone and M. Pozar. Fuel economy benefit of cylinder deactivation - sensitivity to vehicle application and operating constraints. *SAE 2001-01-3591*, 2001.
- [18] Mark McElwee Alan Falkowski and Mike Bonne. Design and development of the daimlerchrysler 5.7l hemi engine multi-displacement cylinder deactivation system. *SAE 2004-01-2106*, 2004.
- [19] J.W.G. Turner K.J. Douglas, N. Milovanovic and D. Blundell. Fuel economy improvement using combined cai and cylinder deactivation (cda) - an initial study. *SAE 2005-01-0110*, 2005.
- [20] Jim Tuttle David Kehr James Westbrook III Henning Karbstein Mark Stabinsky, William Albertson and Mario Kuhl. Active fuel management technology hardware development on a 2007 gm 3.9l v-6 ohv si engine. *SAE 2007-01-1292*, 2007.